4D volcanic geology of Hachijo-jima islet, Izu-Bonin arc

Soichi Osozawa (kawaoso@icloud.com)
KawaOso Molecular Bio-Geology Institute https://orcid.org/0000-0001-5554-1320
Hisatoshi Ito
Central Research Institute of Electric Power Industry
Hiroomi Nakazato
National Agriculture and Food Research Organization
John Wakabayashi
California State University, Fresno

Research Article

Keywords: dissected old volcano, terrestrial and marine volcanic succession, regional tephra, geochronology, ophiolite

Posted Date: April 23rd, 2021

DOI: https://doi.org/10.21203/rs.3.rs-448867/v1

Abstract

This study provides geological, geochemical, and chronological insight into the evolution of the Hachijo-jima volcanoes of the Izu Bonin arc. The regional Ata-Torihama tephra (Ata-Th; 0.24 Ma) and Kikai-Tozurahara tephra (K-Tz; 0.095 Ma) from Kyushu are intercalated within the voluminous proximal volcanic products. Our study combines detailed geologic mapping, tephrochronology, U-Pb zircon dating, and published drill core data from NEDO (1993) to evaluate the time transgressive 3-dimensional (thus 4-dimensional) structure of the dissected Mihara-yama volcano, the older of the two volcanoes on Hachijo-jima. The volcanic succession comprises terrestrial volcanic basement, marine volcaniclastic rocks, and terrestrial tuff intercalated with tholeiitic basalt and the regional calc-alkaline tephra layers. The un-dissected Hachijo-Fuji stratovolcano (tholeiitic basalt) overlies marine volcaniclastics abutting the northwestern paleo sea cliffs of Mihara-yama. Newly-described folding and normal faulting of the marine and overlying terrestrial volcaniclastic rocks suggests NW-SE shortening that may be associated with the collision of the Izu-Bonin arc with the Honshu arc. The proto Hachijo-jima volcano emerged above the sea > 0.24 Ma, and this date can be applied as a molecular biological calibration date for organisms on this island.

Highlight

The erosionally-dissected Mihara-yama volcano was built on 2.1 Ma altered volcanic basement.

Deposition of volcanic strata over this basement buttress unconformity began in submarine conditions at < 1.8 Ma, followed by subaerial pyroclastic flows and a tholeiitic-lava flow from 0.24 Ma onward. Emergence of the Mihara-yama volcano above sea level was > 0.24 Ma.

The Ata-Torihama tephra (Ata-Th; 0.24 Ma; U-Pb age < 0.46 Ma) and Kikai-Tozurahara tephra (K-Tz; 0.095 Ma; U-Pb age < 0.24 Ma) from giant calderas of Ata and Kikai of Kyushu (calc-alkaline) are intercalated in the terrestrial scoriaceous-pumice tuffs derived from the Mihara-yama volcano (tholeiite). Previous correlations to the Aira-Tn tephra (Aira-Tanzawa; AT; 0.0275 Ma) are not viable.

Adjacent to the northwestern paleo sea cliff of this old volcano, a shallow marine basin was formed at < 0.26 Ma. Subaerial scoria and tuff cones were also formed as small-scale lateral volcanoes.

Tholeiitic lava flows built the subaerial Hachijo-Fuji stratovolcano over the shallow marine basin, and two major volcanoes were connected to form a single Hachijo-jima island.

The island deformed by NNW-SSE shortening, reflecting the Izu-Bonin collision toward the central Japan arc.

1. Introduction

Island arcs are among the fundamental geotectonic environments on Earth, and studies of them provide information on plate tectonic mechanisms and history, as well as igneous processes. Whereas most research of island arc geology has focused on petrology, geochemistry, and geochronology of the igneous rocks (e.g., Ishizuka *et al*. 2011, 2018), important new insights into tectonic and igneous processes can be gained by analytical research integrated with detailed geologic mapping (e.g., Busby *et al*. 2018).

This study of volcanic island arc presents detailed geologic mapping and existing subsurface data that provides a necessary foundation for geochemistry and geochronology. The evolution of the volcanic island provides information on global processes, such as volcanostratigraphy and structural evolution of a volcanic island in a context of an island arc approaching arc-arc collision. Detailed field-based studies of modern oceanic island arcs also provide guidance for interpretation of ancient island arc rocks in orogenic belts, including ophiolites interpreted as forming in arc settings (supra-subduction zone ophiolites, e.g., Stern and Bloomer 1992; Shervais 2001; Pearce 2003).

This research also provides information on emergence time of volcanic islands, which is useful for studies of evolution of endemic species that populate such intra oceanic islands. Although this is only a single island, there are few global examples for which the ages of physical emergence or isolation of environments have been geologically determined (Ryukyu continental arc, Osozawa *et al*. 2012a; Panama continental arc, Buchs *et al*. 2019), so just a single age of this sort is of global importance.

2. Regional Setting And Background

From east to west, Izu-Bonin oceanic arc consists of the Bonin ridge representing a fore-arc high, the Ogasawara trough that forms a forearc or intra-arc basin, the Izu volcanic arc, and the Shikoku back-arc basin (Tamura *et al*. 2015; Fig. 1A). The Izu volcanic arc is a Quaternary volcanic island chain lying largely below sea level, and some volcanoes are presently active. Because of the extremely low K content of tholeiitic basalt and young age, reliable K-Ar and Ar-Ar dates have been difficult to obtain, so the age of the basement of this arc has remained uncertain.

The Izu-Bonin arc has long been considered a modern analog for various components of orogenic belts, such as ophiolites with arc petrologic- geochemical signatures (e.g., Stern and Bloomer 1992; Shervais 2001; Pearce 2003; Ishizuka *et al*. 2011; Osozawa *et al*., 2012b). The petrologic and geochemical studies have contributed much to the Izu-Bonin island arcs, but detailed field studies are also important to understand both this arc evolution and to provide more robust comparisons to field relationships observed in ancient orogenic belts.

In addition, oceanic islands provide important information constraining arrival time and evolution animals living on them. Any animal species on such islands must have originally arrived from other land masses through flight or rafting, thus the emergence date of the island is critical to reconstruct their dated phylogeny (Osozawa *et al*. 2016). Until this study, information on the emergence ages of volcanic islands in the Izu-Bonin islands has been lacking, and is also rare globally, including the Aegean islands behind

the Hellenic arc (Papadopoulo *et al*. 2016); such information exists in detail only for islands of the Ryukyu arc (Osozawa *et al*. 2012a).

The present paper focuses on the geology of the Hachijo-jima volcanic island, northern Izu volcanic arc (Fig. 1B; Fig. 2). The island consists of a dissected older Mihara-yama volcano (Fig. 1C, E) and a younger, non-dissected Hachijo-Fuji volcano (Fig. 1C, D). The non-dissected Hachijo-kojima (kojima = small island) volcano lies offshore and west to the Hachijo-Fuji volcano (Fig. 1B). Although dissection of the Mihara-yama volcano is extensive (Fig. 1E), previous studies on this volcano (Isshiki 1959; Tsukui *et al*. 1991, 1993; Suga 1994, 1998; Suga *et al*. 1997; Sugihara, 1998) were based primarily on aerial photo interpretation. The geological map by Sugihara and Shimada (1998) for the younger Hachijo-Fuji volcano appears to be inconsistent with field relationships recorded by detailed geologic mapping of the outcrops. Further, the recently published geological map by the Geological Survey of Japan (Ishizuka and Geshi 2018) is a compilation of the above-referenced studies, so they lack a detailed field geologic foundation including sample locations, photo locations, outcrop descriptions, modes of occurrence (of volcanic rocks), strike and dips of volcanic strata, and stratigraphic relationships.

The dissection of Mihara-yama volcano (Fig. 1E) allows evaluation of internal structure and surface geologic relationships. In contrast, internal structure of a young active volcano such as Hachijo-Fuji volcano (Fig. 1C, D) cannot be observed in surface geologic investigations alone. Core data from kilometer-deep eight borings (Figs. 2 and 3) are available as a result of extensive investigations for geothermal potential reported by NEDO (1993). Such subsurface data is seldom available for a volcano, and the data facilitates characterization of the 3-dimensional (3D) structure of the stratovolcano. Moreover, K-Ar ages of 2.27 ± 4.07 Ma and 0.22 ± 0.06 Ma by NEDO (1993) and 2.12 Ma age by Kaneoka (1970), and marine micropaleontological data giving biostratigraphic ages of < 1.8 Ma and < 0.26 Ma reported in NEDO (1993), are relevant to understanding the history of volcanism (see compilation ages in Fig. 3).

A regional tephra interpreted as the 0.0275 Ma Aira-Tn tephra from the Aira caldera, southern Kyushu (Machida and Arai, 2003; See relevant regional tephra list in Table 1) was reported from the Mihara-yama succession with many radiometric ^{14}C data younger than 0.03 Ma (Sugihara 1998). During our preliminary field observations, it appeared to us that the tephra did not constitute a single layer within the Mihara-yama scoria-pumice tuff successions as previously interpreted. We conducted detailed geological and volcanological analyses to constrain the robust stratigraphic relationships including tephra(s) (Fig. 1 C).

Regional tephras were documented by Machida and Arai (2003), including the distribution and source caldera, shape of glass shards, refractive index, and mineral composition (Table 1). Note that the Aira-Tn (AT) tephra is defined on the basis of its origin from the Aira caldera and the type locality of the tephra Tn (Tanzawa mountains) for example (Table 1), although this naming by Machida and Arai (2003; in Japanese) does not follow the International Stratigraphic Guide. Combined with fission track dating (Danhara, 1995), drill core descriptions (Yoshikawa and Inouchi 1993) and correlation to the oxygen

isotopic curve (Ikehara et al., 2006) and other data, a data table for these regional tephras was constructed (Table 1). However, such regional data should be continually updated with geochronologic and other data. We carried out U-Pb dating by laser ablation-inductively coupled plasma-mass spectrometry (LA-ICP-MS) to the glassy tuffs (tephras) intercalated in the terrestrial strata of the Mihara-yama volcano to provide more robust chronologic correlations.

3. Methods

3.1. Morphological and volcanic geological survey

3D observation of the topographic surface is possible by using 1: 25,000 scale topographic maps (Fig. 1C, Fig. 2 background) and aerial photos (Fig.1D, E) offered by the Geospatial Information Authority of Japan. The relative time relationships of topographic evolution and volcanic deposition, including volcanic development of the Mihara-yama and Hachijo-Fuji volcanoes can be observed with this imagery and topography.

The topology shows severe dissection of the Mihara-yama volcano to the extent that the original edifice has been severely modified (cf., Isshiki 1959; Sugihara 1998; Suga 1998). Whereas this erosional dissection destroys the original edifice shape (Fig. 1E), it enables detailed field geologic investigation because of the 3D exposures afforded by the deep gullies into the volcano.

The field geologic mapping was conducted in the traditional way, integrating outcrop inspection and field identification of rocks with outcrop photography and sketching volcanic-stratigraphic relationships, measurement of contact orientations by compass, identification of key stratigraphic horizons, and the location of key horizons in map view to produce a new geologic map for the volcanoes (Fig. 2). From the geologic mapping, cross sections can be prepared to better evaluate the volcanic stratigraphy and structural geology. Whereas cross sections can be constructed from a geological map, such sections are subject to the assumption the strata observed at surface project beneath the surface at the same orientation. The drill core data of NEDO (1993) gives subsurface information that facilitates construction of more accurate cross sections (Fig. 3).

Previous mapping of the island misidentified some rock types, and distribution and orientations of tilted strata were not given. The proposed Aira-Tn tephra (Sugihara 1998) was not shown by the map distributions nor the sample locations, so these could not be reliably reproduced. Through geological mapping, we identified and mapped two distinct tephra (glassy tuff) layers (Figs. 1C, 2, 3), and did mineralogical and chronological analyses presented below.

3.2. Mineralogy

Minerals including those in the glassy tuffs were observed under stereoscopic microscope and by polarized light microscopy, and identified as well as possible by those methods. Mineral compositions in tephras and pumice (+ obsidian) were analyzed by energy-dispersive spectrometer (EDS) attached to a

scanning electron microscope (Oxford Link ISIS3001 and JEOL JSM-5800LV; Asaki and Yoshida 1999; Osozawa *et al*. 2009; Osozawa and Wakabayashi 2017) at Tohoku University. Sample sites are shown on Figs. 2, 5, and 6E, F. Our preliminary objective was compositional comparison of the white glassy tuff and the yellow pumices and an obsidian in an outcrop of Fig. 5, conducted with the same instrument.

Glass shards in the glassy tuffs were morphologically classified as H (no or few bubbles), C (an intermediate amount of bubbles), and T (many bubbles) types following Yoshikawa (1976). The H type was further classified into Ha (no bubbles) and Hb (with scattered fibrous bubbles), and C and T types were further classified into Ca and Ta (with globular bubbles) and Cb and Tb (with fibrous bubbles).

Refractive index of glass shards included in the lower and upper glassy tuffs, as well as hornblendes included in the lower glassy tuff, was measured by a refractometer called the Measuring Actual Immersion Oil Temperature (Furusawa 1995) in the National Agriculture and Food Research Organization.

3.3. U-Pb dating

Glassy tuffs originally correlated to the Aira-Tn tephra by Sugihara (1998) include zircons, allowing dating by U-Pb methods. Samples were collected from the lower and upper glassy tuffs (HAC-Ata-Th and HAC-K-Tz), and sample sites are shown on Figs. 2, 5, and 6E, F. In addition to zircons from these tephras, we analyzed zircons of Plešovice (Sláma *et al*. 2008), Fish Canyon Tuff (Schmitz and Bowring 2001), and Bishop Tuff (Crowley *et al*. 2007) as secondary standards, and the U-Pb ages obtained were in accordance with the reference values.

Laser ablation-inductively coupled plasma-mass spectrometry (LA-ICP-MS) has been recently widely used for Quaternary tephrochronology (e.g., Guillong *et al*. 2014). Ito (2014) successfully obtained a U-Pb age of the Toya tephra of 0.1 Ma, which indicates that an U-Pb age by LA-ICP-MS can be obtained as young as ~0.1 Ma under favorable conditions. Note that U-Pb dating combined with (U-Th)/He dating suggested protracted periods of zircon crystallization (100's of k.y.) prior to eruption for the Quaternary Omachi tephra, central Japan (Ito and Danišík 2020), and a weighted mean U-Pb age of 0.17 ± 0.05 Ma obtained for the Kikai-Tozurahara tephra in Yaku-shima island (Ito et al. 2017b) was ~70 kyr older than its estimated eruption age of 0.095 Ma (Table 1; Danhara et al. 2010).

LA-ICP-MS U-Pb dating was performed at the Central Research Institute of Electric Power Industry (CRIEPI), using a Thermo Fisher Scientific ELEMENT XR magnetic sector-field ICP-MS coupled to a New Wave Research UP-213 Nd-YAG laser. Data reduction procedures included a Th/U disequilibrium correction assuming a Th/U of magma at 4.0 ± 2.0, and data with high (>75%) common Pb contamination were excluded for further U-Pb analyses. U-Pb ages were calculated following methodology of Sakata (2018). See details of the method in Ito (2014) and Ito and Danišík (2020).

4. Results

4.1. Morphology

The deep dissection of the Mihara-yama volcano observed in aerial photographs (Fig. 1 bottom) obscures the original volcanic landforms such as calderas and sommas (cf., Isshiki 1959; Tsukui *et al*. 1991, 1993; Suga 1994, 1998; Suga *et al*. 1997; Sugihara 1998). The “Koiwato” peninsula with the Koiwatoga-hana cape projects southeastward from the main Mihara-yama volcano without morphological change relative to the main island (Figs. 1 and 2).

Sea cliffs surrounding the Mihara-yama volcano are well developed including around the Koiwato peninsula (Figs. 1B, C and 2). The northwestern cliff is an old sea cliff of an island solely consisting of the northeast base of Mihara-yama, and this paleo sea cliff was later buried by lavas from the newly built Hachijo-Fuji stratovolcano ("former sea cliff" on Fig. 2). The Hachijo-jima airport and Hachijo town area on the island were constructed on these subhorizontal younger lava flows north of the paleo sea cliff. The deep valleys of the northwestern flank represent the mouth of coastal river that was incised into the older Mihara-yama volcano. Small hills surrounded by the Hachijo-Fuji lava flows represent islets offshore the original Mihara-yama main island (Fig. 2). Mt. Kando-yama (Fig. 2) was such an islet, but it was reactivated as a tuff cone and then uplifted.

In contrast to the eroded Mihara-yama volcano, the Hachijo-Fuji volcano lacks erosional dissection and each lava flow radially spreads from the 500-m-diameter crater (Fig. 1C, D; cf., Sugihara, 1998, Ishizuka and Geshi, 2018). The present sea cliff expressed in the younger volcanic materials is much lower (> 5m) compared to those associated the older Mihara-yama coast (Figs. 1C, D and 2).

4.2. Stratigraphy and structure of the Mihara-yama volcano

Scoriaceous tuffs of the main component of the Mihara-yama volcano are well bedded (Fig.4A), and dip to oceanward from the summit of the Mihara-yama up to 30 degrees. The strike lines are concentric around the summit, a typical structure of a stratovolcano. Everywhere on the Mihara-yama edifice, the surface slopes are steeper than the dip of the strata, so stratigraphically higher horizons crop out near the summit whereas stratigraphically lower horizons are exposed in the sea cliffs (Figs. 2 and 3).

Basaltic lavas comprising one to three layers make up the stratigraphically lowest horizons for the main part of the Mihara-yama volcano, and are exposed in most of the sea cliffs (Fig. 2). The basaltic lava flows represent a key bed that can be mapped around the island (Fig. 2). Outcrops of the key basaltic lava are shown on Figs. 4B~D and Fig. 6A~D, G.

Drill holes No. 2 to No. 8 are somewhat randomly located on the Mihara-yama volcano (Fig. 2; NEDO, 1993). Based on the concentric structure of stratovolcano determined from surface geologic mapping, the contact locations in the subsurface can be projected to the section line B-C of cross section of Fig. 3. Fig. 3 shows that the basalt thickens from C (SE coast, Koiwato Peninsula) to B (summit).

A WSW-ENE trending syncline is observed at the base of the Koiwato peninsula, and the key basaltic lava is traceable to the peninsula cliff (Fig. 2). On this peninsula the lowest stratigraphic levels exposed above

sea level crop out; these are horizons below the key basalt layers. These stratigraphically lowest horizons, that are not observed on the main volcanic edifice, are, from top to bottom, a black coarse-grained scoriaceous tuff of 10 m in thickness directly beneath the key basalt, marine volcaniclastic rocks (with cross laminations and with fragments of altered volcanic rocks) including stratified pale yellowish silicic tuffs, and interbedded lavas and tuffs at the base of the sea cliff (Figs. 2 and 3; Fig. 4D~H). These three stratigraphic packages are traceable from the Shioma coast of NE side of the island, the Koiwato-hana cape, and to the Aigae coast of SW side, and constitute key stratigraphic horizons (Fig. 2). The silicic tuffs are asymmetrically folded with SSE vergence, and the folds are observed on opposing coastlines (Shioma and Aigae coasts) (Fig. 4D~G). Along the Aigae coast, NNW-SSE-striking normal faults are observed mostly as conjugate sets (Fig. 2; Fig.4H, I). Isshiki (1959) described a normal fault at the Aigae coast, but mistook the main fault for a sedimentary contact of the base of the recent terrace deposits. A basaltic dike intruded along the normal fault (Fig. 4D).

Drill holes No. 3 and No. 6 penetrated marine volcaniclastic rocks that correspond to the above-mentioned marine strata in the lowest stratigraphic horizon exposed above sea level (Fig. 3). Below this horizon the borings recovered the altered volcanic basement (mostly andesitic; likely marine, considering amygdaloidal texture), but those rocks are not exposed on the land surface (Fig. 3). The basement is directly covered by the key basalt in drill hole No. 2, and No. 4 to No. 8 except for No. 6, and the marine volcaniclastic rocks have pinched out in that area (Fig. 3). All lithological contacts are conformable and there was no clear evidence of unconformities observed in the cores (NEDO, 1993), but there is an onlap relationship of marine and overlying terrestrial strata onto the old volcanic basement (Fig. 3).

Overlying the key basaltic lava is a thick terrestrial accumulation of stratified scoria and pumice tuffs. Sporadic intercalations of basaltic lava are shown on the geological map (Fig. 2). The stratified tuffs (tuff / lapilli tuff / tuff breccia) consist of scoria and some pumice fragments. Pumice is locally predominant and up to boulder size. Grading is commonly observed. These deposits appear to have been deposited as pyroclastic flow, but some horizons appear to have been deposited as debris flows (volcanic sandstone ~conglomerate) and associated with apparent ash fall from the summit.

Two layers of white-colored glassy tuffs are observed, both of which were previously considered a single layer of the Aira-Tn tephra derived from the Aira caldera, southern Kyushu (Sugihara 1988). The lower glassy tuff is found just above the key lava in the sea cliff at the cape Ishizumi-hana where it is 5 cm thick and the frontal cliff of the Sokodo (=Kando) port where it attains 2 m in thickness (Fig. 2). A columnar section and outcrop photos including the lower glassy tuff at the Ishizumi-hana cape are shown in Fig. 5. The glassy tuff is intercalated in pumice dominant tuff layers (= pumice flows; Fig. 5). Additional photos of the lower glassy tuff at the Ishizumi-hana cape are shown in Fig. 6A, B, and photos at the Sokodo port are shown in Fig. 6C, D. The upper glassy tuff is observed at 170 m in altitude (Figs. 2 and 3), and stratigraphically overlies the lower glassy tuff at 0 m in altitude by approximately ~ 170 m thickness, taking into account the dip of ~10 degrees. Photos of the upper glassy tuff are shown in Fig. 6E, F, and the tuff is also intercalated in pumice rich tuff but with volcanic fragments. These tuffs are partly asymmetrically folded with NW vergence and displaced by a thrust fault to the right of Fig. 6E.

In Fig. 6E, pumice tuff/tuff breccia is weathered and soft, but hard fresh tuff is exposed near the valley, so that the original fresh rock is not a soft and unconsolidated sediment composed of airfall pumice (pumice itself is a fibrous glass shard and originally consolidated). Stream potholes are eroded into the resistant black scoria and glassy tuff (Figs. 2 and 7). Under thin section, the matrix is glass, and plagioclase and pyroxene are anhedral (Fig. 7), in contrast to euhedral crystals in basaltic lava cropping out to the NE (Fig. 2). The tuff lacks welded texture (Fig. 7). The type Aira-Tn tephra is an unconsolidated loam (e.g., Kosaka *et al*. 2014), and potholes cannot form in unconsolidated sediments; they can only form in erosionally resistant rock.

4.3. Scoria cone and tuff cone

The Kurozuna scoria cone is on the rim of the SW sea cliff of the Mihara-yama volcano (Fig. 2). “Kurozuna” in Japanese means black sands, and consists of unconsolidated scorias of granule to pebble size. This vent is close to the sea cliff edge, so colluvial sand covers the top of the sea cliff that consists of the key basaltic lavas and tuffs (Fig. 6G). Due to its interesting appearance and setting, “Kurozuna” is frequented by sightseers but is dangerous owing to the loose material perched on the cliff edge (Fig. 6G); in spite of its popularity with tourists it was only recently reported by Ishizuka and Geshi (2018).

Mt. Kando-yama, on the southeastern flank of the Hachijo-Fuji volcano, consists of shallow to moderately-dipping bedded scoriaceous tuffs, and the lithology is the same as the terrestrial scoriaceous tuffs widespread on the southeastern Mihara-yama volcano (Fig. 2). Two circular depressions representing two craters are observed at the NE-SW trending anticlinal core (Fig. 2), and these are filled by unconsolidated scoria of granule to pebble size. The scoria overlies unconsolidated talus deposits (Fig. 6H), and underlies the Hachijo-Fuji lava (at this outcrop, the scorias associated with lava breccia).

4.4. Stratigraphy and structure of the Hachijo-Fuji volcano

Hachijo-Fuji volcano has a crater of 500 m in diameter, with lavas making up the crater walls and the flanks of the volcano. Basaltic lavas are mostly pahoehoe (Fig. 6I). Lavas are best observed in sea cliff on the NW side of the Hachijo-Fuji volcano, and the strata dip gently seaward, similar to the Mihara-yama volcano, but the dip angle equals to the slope angle for Hachijo-Fuji. Lavas along the SE flank have flat dip, and these apparently buried a paleo shallow sea and reached the NW sea cliff of the Mihara-yama volcano. As noted, the airport, town area, and also the NE side Sokodo port and the SW side Yaene port were built on these relatively flat lava flows (Fig. 2).

Drill hole No. 1 near the airport (Fig. 2) penetrated the Hachijo-Fuji basalt, then terrestrial volcaniclastics beneath the lava flows, marine unconsolidated volcaniclastics, and marine consolidated volcaniclastic rocks probably correlated to those of the Shioma coast, SE of the Mihara-yama volcano (Fig. 3; NEDO 1993).

4.5. Geochemistry of glassy tuffs (Table 2)

Stereoscopic microscopic examination showed that both the lower and upper glassy tuffs consist primarily of glass shards. Bubbles in glass shards are not common, with an order of Ha and Hb>Cb>Tb. The upper glassy tuff contains high quartz (β-quartz) as well as plagioclase fragments, but the lower glassy tuff does not contain quartz, and both tuffs contain mafic minerals.

The glass composition for the lower glassy tuff (HAC-Ata-Th) is 77-78 % SiO2, 1.2-1.5 % FeO, 0.12-0.16 % MgO, and 3.4-3.6 % K2O. The glass composition for the upper glassy tuff (HAC-K-Tz) is 78 % SiO2, 1.2-1.5 % FeO, and 0.12-0.18 % MgO, and 3.3-3.5 % K2O similar to HAC-Ata-Th.

Glass composition for pumice and obsidian (HAC-LP-pumice, HAC-UP-pumice, HAC-OBC-obsidian) is 73-75 % SiO2, 4.1-5.2 % FeO, 0.47-0.75 % MgO, and 0.95-1.05 % K2O distinct from that of the upper and lower glassy tuffs. High quartz (β-quartz) is observed in HAC-LP-pumice and HAC-UP-pumice; some is visible macroscopically.

These glass composition data combined with published tephra data were plotted on a SiO2-K2O diagram (Fig. 8). Data of the Ata-Th and K-Tz tephras plot within calc-alkaline series, and those of HAC-LP-pumice, HAC-UP-pumice, HAC-OBC-obsidian plot within tholeiite series.

We confirmed that the mafic mineral is hornblende (HAC-Ata-Th-hornblende) in the lower glassy tuff, and orthopyroxene (HAC-K-Tz-orthopyroxene) and clinopyroxene (HAC-K-Tz-clinopyroxene) in the upper glassy tuff.

We obtained similar range of refractive index of glass shards of the lower and upper glassy tuffs (HAC-Ata-Th-glass, HAC-K-Tz-glass), and the refractive index of hornblendes of the lower glassy tuff (HAC-Ata-Th-hornblende).

4.6. U-Pb age (Table 3)

We obtained U-Pb ages from zircons of the lower and upper glassy tuffs (HAC-Ata-Th and HAC-K-tz), although HAC-LP-pumice, HAC-UP-pumice, and silicic tuff of Fig. 4G contain no zircon.

U-Pb dates from the lower glassy tuff zircons (HAC-Ata-Th) were mostly < 4 Ma with some xenocrystic > 15 Ma zircons (Table 3). Taking a weighted mean age of all < 4 Ma zircons yields an age of 0.88 ± 0.21 Ma (95% confidence; n = 15; MSWD = 10.3) (Fig. 9). The large MSWD indicates that these zircons may contain xenocrysts and/or antecrysts (Miller *et al.* 2007). In this case, youngest zircons likely represent the eruption date, although they still should be regarded as a maximum estimate for the eruption age. Consequently, we selected the youngest 3 zircons to represent the eruptive age, giving a weighted mean age of 0.46 ± 0.12 Ma (MSWD = 0.44). Although an age of 0.36 (+0.16, -0.19) Ma was calculated by the 'youngest detrital zircon' routine in Isoplot program (Ludwig 2012), we assume that the lower glassy tuff erupted at 0.46 ± 0.12 Ma.

The upper glassy tuff zircons (HAC-K-tz) yielded predominantly ages of < 3 Ma with one ~14 Ma (Table 3). A weighted mean age of all < 3 Ma zircons is calculated as 0.41 ± 0.33 Ma (n = 10; MSWD = 13).

Because of a large MSWD value, we selected the youngest 4 zircons, which yielded a weighted mean age of 0.24 ± 0.09 Ma (MSWD = 0.48). Although an age of 0.08 (+0.16, 0.9) Ma is calculated by the 'youngest detrital zircon' routine in Isoplot program (Ludwig 2012), we tentatively assume that the upper glassy tuff erupted at 0.24 ± 0.09 Ma.

5. Discussion

5.1 Correlation to the regional tephras

Both the lower and upper tuffs mostly consist of glass shards associated with more or less bubbles, and should have originated from subaerial ash falls derived from some of the giant calderas of western Japan. Note that winds blowing from the west prevail in the middle latitudes of northern hemisphere, including Japan and the Hachijo-jima island. Pumices and obsidians (HAC-UP, HAC-LP, HAVC-OBC) have lower and distinct K2O contents than the glass shards of the white colored lower and upper glassy tuffs (HAC-Ata-Th, HAC-K-Tz), and were directly derived from the Mihara-yama volcano, in contrast to the “exotic” glass shards in regional tephras (HAC-Ata-Th, HAC-K-Tz). Pumices and obsidians (HAC-UP, HAC-LP, HAVC-OBC) are plotted in the tholeiite field (Fig. 8) as for the Mihara-yama lavas (Tsukui et al., 1993; Suga et al., 1997) and the Hachijo-Fuji lavas (Nakano *et al*. 1991; Tsukui and Hoshino 2002), and the glass shards of the lower and upper tuffs including HAC-Ata-Th, and HAC-K-Tz are plotted in the calc-alkaline field (Fig. 8).

The Izu-Bonin volcanic arc initiated activity at ca. 48 Ma for the Chichi-jima island (Ar-Ar dating; Ishizuka et al., 2006) and ca. 51 Ma for the Bonin Ridge (Ar-Ar dating; Ishizuka et al., 2011), and was an immature arc not yet generating mature granitic crust. Zircon xenocrysts as old as 200 Ma obtained from the glassy tuffs (Table 3) are not expected for the relatively young Izu-Bonin arc (although dredged basalts yielded some exceptional Ar-Ar ages of 159 Ma; Ishizuka *et al*. 2011). In constrast, eruption with old xenocrystic zircons would be expected from volcanoes in the Japan-Ryukyu arc, which has old and mature continental basement.

The lower and upper tuffs should be correlated with two distinct regional tephras whose ages should be younger than 0.46 ± 0.12 Ma (weighted mean age of the lower glassy tuff; Fig. 9). Machida and Arai (2003) studied and compiled regional tephras from the Kyushu giant calderas (Table 1), and the Kakuto (0.335 Ma), Aso-1 (0.26 Ma), Ata-Torihama (0.24 Ma), Ata (0.107 Ma), Kikai-Tozurahara (0.095 Ma), Aso-4 (0.0875 Ma), Aira-Tn (Aira-Tanzawa; 0.0275 Ma), and Kikai-Ah (Kikai-Akahoya; 0.0073 Ma) tephras are viable candidates based on age (ages after Danhara et al., 2010). Mt. Sanbe (alkaline), Daisen (alkaline), Tateyama (calc-alkaline), Ontake (calc-alkaline), and Fuji (tholeiite) and Hakone (calc-alkaline) (Fig. 10) are not candidates because of the prevailing west winds.

Discrimination between alternative tephras is relatively easy, because hornblende as the only mafic mineral is a characteristic of only the Ata-Torihama tephra (hornblende refractive index is also similar; see Table 2), and high quartz (β-quartz) inclusions are a characteristic of the Kikai-Tozurahara tephra (Machida and Arai 2003). Accordingly, we correlate the lower glassy tuff to the Ata-Torihama tephra and

the upper glassy tuff to the Kikai-Tozurahara tephra, although glass compositions of such as SiO2 and K2O are similar among various tephras and glassy tuffs, including the Aira-Tn tephra (Table 2; Fig. 8). Note that although major element geochemical data are not distinctive among tephras, the Kakuto, Ata, and Aso-4 tephras have distinct compositions (Table 2; Fig. 8). In addition, the refractive index of glass is similar among these tephras and glassy tuffs including the Aira-Tn tephra (Table 2) and hence does not distinguish these tephras, although it is distinct for the Kakuto, Ata, and Aso4 tephras (Table 2). A glass refractive index was reported in Sugihara (1998; no sample location data) and a glass chemical composition was given in Tsukui et al. (1991; no sample location data), which misled these authors to correlate the glassy tuff(s) with the Aira-Tn tephra. Refractive index of HAC-Ata-Th-hornblende from the lower glassy tuff was also similar to those of the Ata-Th tephra from other localities (Table 2).

5.2. Tephrochronology combined with the present U-Pb dating

Ages of the correlated regional tephras of Ata-Torihama (0.24 Ma) and the Kikai-Tozurahara (0.095 Ma) were already inferred and available to apply to the ages of the lower and upper glassy tuffs (HAC-Ata-Th, HAC-K-Tz) intercalated in the terrestrial stratigraphy of the Mihara-yama volcano. In detail, age estimation of these regional tephras was done combining radioisotopic dates with oxygen isotopic stratigraphy, estimate of sedimentation rate, and marine micropaleontology (Yoshikawa and Inouchi 1993; Nagahashi *et al*. 2004; Ikehara *et al*. 2006; Aoki *et al*. 2008; Danhara *et al*. 2010; Domitsu *et al*. 2010). The above age estimates, however, primarily rely on the zircon fission track ages of 0.24 ± 0.04 Ma for the Ata-Torihama tephra and 0.098 ± 0.026 Ma (later modified to 0.095 Ma in Danhara *et al.* 2010) for the Kikai-Tozurahara tephra (Danhara 1995). Danhara (1995) noted that for the Kikai-Tozurahara tephra, the total numbers of zircons with fission tracks were only 14 of 144 zircons, with 130 zircons lacking fission tracks.

Ito (2014), Ito et al. (2017a, b), and Ito and Danišík (2020) attempted to estimate more reliable U-Pb ages of the Quaternary (but younger than 1 Ma) regional tephras in Japan than the previously-applied fission track dating. Whereas Sugihara (1998) misinterpreted the glassy tuffs as the Aira-Tn tephra (0.0275 Ma), he presented many radiocarbon ages for lignite fragments contained in the Mihara-yama strata (a dated lignite sample may be from that near HAC-UP in Fig. 5), but his data cannot be reliably used in the absence of a robust field stratigraphic context.

Our zircon analyses obtained a weighted mean U-Pb age of the lower glassy tuff (HAC-Ata-Th) at 0.46 ± 0.12 Ma, which is older than the widely-accepted Ata-Torihama age of 0.24 Ma. Although it is difficult to obtain the eruption date precisely by the zircon U-Pb method (Ito and Danišík 2020), the obtained U-Pb age can constrain that the tephra is younger than ~0.5 Ma. Accordingly, the obtained age is consistent with the lower glassy tuff being the Ata-Torihama.

A weighted mean zircon U-Pb age of the upper glassy tuff (HAC-K-Tz) was obtained at 0.24 ± 0.09 Ma, younger than the lower glassy tuff. From mineralogical perspectives as mentioned above, we correlate this tephra the Kikai-Tozurahara. Ito et al. (2017b) obtained a zircon U-Pb age of 0.17 ± 0.05 Ma from the Kikai-Tozurahara tephra in the Yaku-shima island, Kyushu, concordant with the present result. The obtained U-Pb age supports the correlation of the upper glassy tephra as the Kikai-Tozurahara.

5.3. 4D volcanic geology (Fig. 3)

The evolution of the Hachijo-jima volcanoes in relative time is illustrated by the cross sections that show the 3D stratigraphic relationships. Structure and succession of the Mihara-yama volcano is symmetric relative to the section, as illustrated by the concentric strike lines around the summit, constituting a typical radial structure of a stratovolcano. Accordingly, its evolution can be evaluated in 2D map or cross sectional views for 3D structure, and this analysis expands to 4D with consideration of chronologic relationships. The Hachijo-Fuji volcano represents a typical and not dissected stratovolcano similar to the Fuji volcano (Fig. 10), and the 3D structure is simple.

The submarine volcanic basement of the Mihara-yama volcano consists of altered volcanic and volcaniclastic rocks, dated by K-Ar methods at 2.12 Ma (Kaneoka *et al*. 1970) and 2.27 ± 4.07 Ma (NEDO 1993), and that may have formed an andesitic submarine volcano. Marine volcaniclastic rocks were deposited at the foot of the submarine volcano with buttress unconformity and fragments of altered volcanic rocks are included within the lowermost marine volcaniclastic strata overlying the basement. The above 2.12 Ma K-Ar age by Kaneoka *et al*. (1970) was obtained from a sample of such a volcanic clast. The originally submarine basement edifice would have later uplifted and emerged above sea level when the marine volcaniclastic rocks were accumulated.

The date of the lower glassy tuff correlated to the Ata-Torihama tephra is 0.24 Ma, and the lower tuff is slightly above the key basaltic lava flow stratigraphically (Fig. 5, Fig. 6 A-D). This terrestrial basaltic volcanism (dated by K-Ar method at 0.22 ± 0.06 Ma by NEDO 1993; Fig. 3) mostly comprising lava flows began at this time of 0.24 Ma, and these horizons conformably overlie terrestrial tuffs but locally abut the altered volcanic basement near the eruption center with unconformity (see Fig. 3). The basaltic key lava underlies key submarine scoriaceous tuff in outcrops of the Shioma and Aigae coasts, which might be a precursor of voluminous terrestrial scoria and pumice flows and falls.

Shortly after eruption of the key basaltic lava flows, the Ata-Torihama tephra of 0.24 Ma derived from the Ata caldera, Kyushu (Fig. 10), was deposited and intercalated in the pumice flows derived from the Mihara-yama volcano. A later tephra of the Kikai-Tozurahara at 0.095 Ma was derived from the Kikai caldera, Kyushu (Fig. 10), and also intercalated in the pumice flows derived from the Mihara-yama volcano. The thickness of scoria and pumice tuffs between the two tephra horizons is < 170 m, and the sedimentation rate is estimated of < 1.14 mm/y. This accumulation rate is an order of magnitude faster than that of the Lake Biwa sediments (Yoshikawa and Inouchi 1993), and may be reasonable for volcanic- pyroclastic successions. Note that the Kikai-Tozurahara tephra observed at the front of the Sokodo port is 2 m in thick (Fig. 6 C, D), possibly a drift of ash. Tokyo is also distant from Kyushu caldera (Fig. 10), but may need to consider hazards associated with such ash drift.

We observed the SSE vergent asymmetric folds (and also thrust fault associated with NW-vergent asymmetric fold) and the NNW-SSE trending conjugate sets of normal faults, and these structures indicate NNW-SSE compressive stress axis. The Hachijo-jima island deformed by the NNW-SSE shortening, reflecting the Izu-Bonin collision toward the central Japan arc (Suga 1998).

After the effusive and explosive volcanism of Mihara-yama ceased, a scoria cone was formed at the SW foot of the Mihara-yama, and formed the Kurozuna scorias. The Kando-yama tuff cone that formed offshore and NW of Mihara-yama also deposited scorias.

Margin of the Mihara-yama volcano was eroded by wave action so that a sea cliff formed surrounding the volcanic island. To the NW there was shallow sea, and the drill hole No. 1 cored unconsolidated marine volcaniclastics there (associated consolidated strata at the bottom; Fig. 3). Above this unit, the core exhibits unconsolidated terrestrial volcaniclastics, that covered the marine sediments as a precursor of the main stage Hachijo-Fuji volcanism and filled the shallow sea (Fig. 3). The main lava flows accumulated to form the Hachijo-Fuji stratovolcano, and some lavas abutted the preexisting Mihara-yama sea cliff and the Kando-yama tuff cone.

The emergence of Hachijo-jima above sea level as an island took place by 0.24 Ma when deposition of the terrestrial tuff and its intercalated Ata-Torihama tephra began. However, marine volcaniclastic rocks abutted the altered volcanic basement along a buttress unconformity, and the basement may have been uplifted to form a subaerial summit between 2.12 Ma and 0.24 Ma. The emergence time is thus not well constrained, but if we apply the above estimated sedimentation rate of 1.14 mm/y to the 750 m layer between the base of key basaltic lava and the base of marine volcaniclastic rocks (Fig. 3), the duration of sedimentation was 0.65 m.y., and the emergence age as an island is calculated as 0.24 + 0.65 = 0.89 Ma. However, the date is conservatively constrained as > 0.24 Ma. The emerged island area is estimated to be only 10 km^2 at 0.89 Ma (Table 4), and the habitat may be small to support land organisms. Such a date is useful for calibration of molecular biologic events associated with the islands of the Izu-Bonin arc (Osozawa et al., 2021); similar sorts of geologic calibration for molecular biology have been applied by Osozawa et al. (2012a).

5.4. Implications for genesis of the Troodos ophiolite

Although trace element and isotopic data are lacking for the Mihara-yama basalt as well as the Hachijo-Fuji basalts, the present geological and chronological data allows comparison with other island arc terranes, including those interpreted as supra subduction zone ophiolites (e.g. Stern and Bloomer 1992; Shervais 2001; Pearce 2003), and facilitates comparisons of the genesis of units such as the Troodos ophiolite of Cyprus (Osozawa *et al*. 2012b).

For the Troodos ophiolite island-arc tholeiite of the lower pillow lava sequence erupted first, followed by boninite (Osozawa *et al*. 2012b). The trace element and REE composition of the Troodos arc tholeiite patterns closely resemble typical intra-oceanic-arc tholeiite of the Izu-Bonin arc (O-shima basalt named JB2, and Haha-jima basalt of the Bonin Ridge; Fig. 1) and of the Mariana forearc, although the “U-shaped” REE pattern of Troodos boninite differs markedly from the type boninite from Chichi-jima of the Bonin Ridge.

Our biostratigraphic data from the Troodos ophiolite indicate that most of the basal pelagic sedimentary rocks that conformably overlie the boninitic rocks are ca. 75 Ma (Osozawa *et al*. 2012b). This suggests

that voluminous eruption of boninitic rocks persisted until ca. 75 Ma, since 90.6 ± 1.2 Ma (Ar-Ar age, but limited eruption of boninitic lavas may have continued until 55.5 ± 0.9 Ma). The duration of arc magmatism at Troodos was at least 16 m.y., with some activity perhaps extending 35 m.y. without the development of a mature arc edifice. Such extended magmatism long is recorded in the Bonin Ridge with duration up to ca. 15 m.y. (Ishizuka *et al*. 2011) or ca. 51-49 m.y., if the eruptive duration includes the active or the presently addressed 2.1 Ma volcanism. A schematic columnar section to summarize of the Bonin Ridge forearc section was shown in figure 4 in Ishizuka et al. (2011), and the ophiolitic sequence was reconstructed as peridotite, gabbro, sheeted dyke, and basalt including island-arc tholeiite and boninite, similar to the Troodos ophiolite sequence.

A part of deep sea sediment cover over the Troodos pillow lavas is called the Kannaviou Formation consisting of silicic tuff (Robertson 1977; Osozawa and Okamura 1993). The silicic tuff might have derived from a mature island arc distinct from the nascent suprasubduction-zone setting (Robertson 1977). From implications from the present study, the Mihara-yama succession, including tholeiitic lavas formed in a young immature island arc, contains the exotic calc-alkaline tephras derived from the Kyushu calderas of a mature volcanic arc, a relationship similar to the cover of the Troodos ophiolite. Alteration of the Hachijo lavas and Troodos lavas is very mild, and unaffected by deformation such as pressure solution cleavage. We found ENE-WSW syncline and outcrop scale asymmetrical faults from Hachijo-jima, and the WNW-ESE anticlinal dome from the Troodos ophiolite is well documented (Osozawa *et al*. 2012). Both reflect obduction or pre-collisional shortening event as an immature subduction zone approached a mature one.

6. Conclusions

The erosionally-dissected Mihara-yama volcano was built on 2.12 Ma submarine volcanic basement. The deposition of volcaniclastic strata over this basement by buttress unconformity began in submarine conditions at < 1.8 Ma, and was succeeded by terrestrial pyroclastic flows and a tholeiitic-lava flow from 0.24 Ma onward. Emergence of the Mihara-yama volcano above sea level was > 0.24 Ma (ca. 0.89 Ma). The Ata-Torihama tephra (Ata-Th; 0.24 Ma; U-Pb age < 0.46 Ma) and Kikai-Tozurahara tephra (K-Tz; 0.095 Ma; U-Pb age < 0.24 Ma) from giant calderas of Ata and Kikai of Kyushu (calc-alkaline) are intercalated in the terrestrial scoriaceous-pumice tuffs in the Mihara-yama volcano (tholeiitic). Adjacent to the northwestern paleo seacliff of this old volcano, a shallow marine basin was formed at < 0.26 Ma. Subaerial scoria and tuff cones were also formed as small-scale lateral volcanoes. Tholeiitic lava flows built the subaerial Hachijo-Fuji stratovolcano over the shallow marine basin, and two major volcanoes were connected to form a present, single Hachijo-jima island. The island deformed by NNW-SSE shortening, reflecting the Izu-Bonin collision toward the central Japan arc, comparable to the NNE-SSW shortening observed for the Troodos ophiolite. The silicic tuff cover of the ophiolite may be analogy of the regional tephra derived from the adjacent but mature volcanic arc.

Declarations

Acknowledgements

The field survey was partly financially supported by the Hachijojima Tourist Association and Hachijo Island Geothermal Energy Museum, and we thank Yuichi Oba, Yumiko Oba, and Tsutomu Shimada for the invitations of the first author to the Hachijo-jima island. Yoshinori Ito assisted with EDS analyses, and Michiaki Abe made thin sections.

Competing interests

The authors declare no competing interests.

References

Aoki, K., Irino, T., and Oba, T, 2008, Late Pleistocene tephrostratigraphy of the sediment core MD01-2421 collected off the Kashima coast, Japan. The Quaternary Research, v. 47, p. 391–407. (in Japanese with English abstract)

Asaki, T., and Yoshida, T., 1999, Alterration of basalts from the Shimanto belt in southern Tokushima Prefecture, Southwest Japan. Japanese Journal of Petrology, Mineralogy, and Economic Geology, v. 94, p. 11-36. (in Japanese with English abstract)

Busby, C.J., Putirka, K., Melosh, B., Renne, P.R., Hagan, J.C., Gambs, M., and Wesoloski, C., 2018, A tale of two Walker Lane pull-apart basins in the ancestral Cascades arc, central Sierra Nevada, California: Geosphere, v. 14, p. 1-50. https://doi.org/10.1130/GES01398.1.

Crowley, J.L., Schoene, B., and Bowring, S.A., 2007, U-Pb dating of zircon in the Bishop Tuff at the millennial scale. Geology, v. 35, p. 1123–1126.

Danhara, T., 1995, Towards precise measurement of zircon and glass fission-track geochronology for Quaternary tephras. The Quaternary Research, v. 34, p. 221–237. (in Japanese with English abstract)

Danhara, T., Yamashita, T., Iwano, H., Takemura, K., and Hayashida, A., 2010, Chronology of the 1400-m core obtained from Lake Biwa in 1982–1983: Re-investigation of fission-track ages and tephra identification. The Quaternary Research, v. 49, p. 101–119. (in Japanese with English abstract)

Domitsu, H.， Nishi, H.， Uchida, J.， Oda, M.， Ogane, K.， Taira, A.， Aoike, K., and Shimokita Microfossil Research Group, 2010, Age model of core sediments taken by D/V CHIKYU during the shakedown cruises off Shimokita Peninsula. Fossils, v. 87，p. 47–64. (in Japanese with English abstract)

Furusawa, A., 1996, Identification of tephra based on statistical analysis of refractive index and morphological classification of volcanic glass shards. Journal of Geological Society of Japan, v. 101, p. 123–133. (in Japanese with English abstract)

Guillong, M., von Quadt, A., Sakata, S., Peytcheva, I., Bachmann, and O., 2014, LA-ICP-MS Pb-U dating of young zircons from the Kos-Nisyros volcanic centre, SE Aegean arc. The Journal of Analytical Atomic Spectrometry, v. 29, p. 963–970.

Ikehara, M., Murayama, M., Tadai, O., Hokanishi, N., Daido, N., Kawahata, H., and Yasuda, H, 2006, Late Quaternary tephrostratigraphy of two IMAGES cores taken from the off Shikoku in the Northeast Pacific. Fossils, v. 79, p. 60–76. (in Japanese with English abstract)

Ishizuka, O., and Geshi, N, 2018, Geological map of Hachijojima Volcano. Geological Map of Volcanoes, no. 20, Geological Survey of Japan, AIST.

Ishizuka, O., Kimura, J., Li, Y. B., Stern, R. J., Reagan, M. K., Taylor, R. N., Ohara, Y., Bloomer, S. H., Ishii, T., Hargrove III, U. S., and Haraguchi, S, 2006, Early stages in the evolution of Izu-Bonin arc volcanism: new age, chemical, and isotopic constraints. Earth and Planetary Science Letters, v. 250, p. 385–401.

Ishizuka O, Tani K, Reagan MK, Kanayama K, Umino S, Harigane Y, Sakamoto I, Miyajima Y, Yuasa M, and Dunkley DJ., 2011, The timescales of subduction initiation and subsequent evolution of an oceanic island arc. Earth and Planetary Science Letters, v. 306, p. 229–240.

Ishizuka O, Hickey-Vargas R, Arculus RJ, Yogodzinski GM, Savov IP, Kusano Y, McCarthy A, Brandl PA, and Sudo M., 2018, Age of Izu–Bonin–Mariana arc basement. Earth and Planetary Science Letters, v. 481, p. 80–90.

Isshiki, N., 1987, Geology of the Hachijojima district. quadrangle series scale 1: 50,000, Geological Survey of Japan, 58pp. (in Japanese with English abstract)

Ito, H., 2014, Zircon U–Th–Pb dating using LA-ICP-MS: Simultaneous U–Pb and U–Th dating on the 0.1 Ma Toya Tephra, Japan. Journal of Volcanology and Geothermal Research, v. 289, p. 210–223.

Ito, H., Nanayama, F, and Nakazato, H, 2017a, Zircon U–Pb dating using LA-ICP-MS: Quaternary tephras in Boso Peninsula, Japan. Quaternary Geochronology, v. 40, p. 12–22.

Ito, H., Uesawa, S., Nanayama, F., and Nakagawa, S, 2017b, Zircon U–Pb dating using LA-ICP-MS: Quaternary tephras in Yakushima Island, Japan. Journal of Volcanology and Geothermal Research, v. 338, p. 92–100.

Ito, H., and Danišík, M, 2020, Dating late Quaternary events by the combined U-Pb LA-ICP- MS and (U-Th)/He dating of zircon: A case study on Omachi Tephra suite (central Japan). Terra Nova, v. 32, p. 134–140.

Kaneoka, I., Isshiki, N., and Zashu, S., 1970, K-Ar ages of the Izu-Bonin Islands. Geochemical Journal, v. 4, p. 53–60.

Kosaka, H., Miwa, A., Imaizumi, T., Inagaki, H., Hashimoto, S., Kagohara, K., and Sasaki, A., 2014, Fault exposure of Dainenjiyama fault across urban district of Sendai City, Northeast Japan. Journal of the Japan Society of Engineering Geology, v. 55, p. 166–176. (in Japanese with English abstract)

Kasama, T., and Shioi, H, 2019, Stratigraphic subdivision of the Pleistocene Miyata Formation based on lithology and unconformity, Miura Peninsula, with special reference to the radiometric age of the intercalated Funakubo Tuff. Bulletin of Kanagawa prefecture Museum (Natural Sciences), v. 48, p. 1–12. (in Japanese with English abstract)

Ludwig K.R., 2012, User's Manual for Isoplot 3.75: A geochronological Toolkit for Microsoft Excel. Berkeley Geochronology Center Special Publication, no. 5, 75 p.

Machida, H. and Arai, F., 2003, Atlas of tephra in and around of Japan. Tokyo University Press, Tokyo, 336 p. (in Japanese)

Miller, J.S., Matzel, J.E.P., Miller, C.F., Burgess, S.D., and Miller, R.B., 2007, Zircon growth and recycling during the assembly of large, composite arc plutons. Journal of Volcanology and Geothermal Research, v. 167, p. 282–299.

Nagahashi Y., Yoshikawa, S., Miyakawa, C., Uchiyama, T., and Inouchi, Y., 2004, Stratigraphy and chronology of widespread tephra layers during the past 430 ky in the Kinki District and the Yatsugatake Mountains: Major element composition of the glass shards using EDS analysis. The Quaternary Research, v. 43, p. 15–35. (in Japanese with English abstract)

Nagahashi, Y., Sato, T., Takeshita, Y. Tawara, T., and Kumon, F., 2007, Stratigraphy and chronology of widespread tephra beds intercalated in the TKN-2004 core sediment obtained from the Takano Formation, central Japan. The Quaternary Research, v. 46, p.305-325. (in Japanese with English abstract)

Nagahashi, Y., and Kataoka, K.S., 2014, Tephrology (part 5) : Major element composition of volcanic glass shards and tephra beds correlation. The Quaternary Research, v. 53, p. 265—270. (in Japanese with English abstract)

Nakano, S., Yamamoto, T., and Ishhiki, N., 1991, Major-element chemistry of Nishiyama volcano, Hachijojima. Japanese Journal of Petrology, Mineralogy, and Economic Geology, v. 86, p. 72-81. (in Japanese with English abstract)

Nakazato, H., and Sato, H., 2016, Stratigraphy of the Shimosa Group in the northern part of Chiba Prefecture, v. 71, p. 55–78. (in Japanese with English abstract)

NEDO, 1993, Reports of development of geothermal power, Hachijo-jima 32, 1202 p. (in Japanese with English abstract)

Ooi, S., 2013, Stratigraphy and tephro-stratigraphy of the Quaternary Shimosa Group in Hitachi Terrace. http://hdl.handle.net/10109/4700 (in Japanese with English abstract)

Osozawa, K., Ogino, S., Osozawa, S., Oba, Y., and Wakabayashi, J., 2016, Carabid beetles (*Carabus blaptoides*) from Nii-jima and O-shima isles, Izu-Bonin oceanic islands: Dispersion by Kuroshio current and the origin of the insular populations. Insect Systematics & Evolution, v. 46, p. 1–16.

Osozawa, S., and Okamura, M., 1993, New radiolarian ages from theTroodos ophiolite and their tectonic implications. The Island Arc, v. 2, p. 1–6.

Osozawa, S., Morimoto, J., Flower, M.F.J. 2009. “Block-in-matrix” fabrics that lack shearing but possess composite cleavage planes: A sedimentary mélange origin for the Yuwan accretionary complex in the Ryukyu island arc, Japan. Geological Society of America Bulletin, v. 121, p. 1190–1203.

Osozawa, S., Shinjo, R., Armig, R., Watanabe, Y., Horiguchi, T., and Wakabayashi, J., 2012a, Palaeogeographic reconstruction of the 1.55 Ma synchronous isolation of the Ryukyu Islands, Japan, and Taiwan and inflow of the Kuroshio warm current. International Geology Review, v. 54, p. 1369-1388.

Osozawa, S., Shinjo, R., Lo, C.H., Jahn, B., Hoang, N., Sasaki, M., Ishikawa K., Kano, H., Hoshi, H., Xenophontos, C., and Wakabayashi, J., 2012b, Geochemistry and geochronology of the Troodos ophiolite: An SSZ ophiolite generated by subduction initiation and an extended episode of ridge subduction? Lithosphere, v. 4, p. 497–510.

Osozawa, S., and Wakabayashi, J., 2017, Variety of origins and exhumation histories of Sambagawa eclogite interpreted through the veil of extensive structural and metamorphic overprinting. In Bianchini, G., Bodinier, J.-L., Braga, R., Wilson, M., eds., The Crust-Mantle and Lithosphere-Asthenosphere Boundaries: Insights from Xenoliths, Orogenic Deep Sections, and Geophysical Studies: Geological Society of America Special Paper, no. 526, p. 49–71.

Osozawa, S., Kanai, K., Fukuda, H., and Wakabayashi, J., 2021, Phylogeography of Ryukyu insular cicadas: Extensive vicariance by island isolation vs accidental dispersal by super typhoon. PlOS ONE.

Papadopoulo, A., Anastasiou, I., and Vogler, A.P., 2010, Revisiting the insect mitochondrial molecular clock: The mid-Aegean trench calibration. Molecular Biology and Evolution, v. 27, p. 1659–1672.

Pearce, J.A., 2003, Supra-subduction-zone ophiolites: the search for modern analogues. In: Dilek, Y., and Newcomb. S. eds. Ophiolite Concept and the Evolution of Geologic Thought. Geological Society of America Special Paper, no. 373, p. 269-294.

Robertson, A.H.F., 1977, The Kannaviou Formation, Cyprus: Volcaniclastic sedimentation of a probable Late Cretaceous volcanic arc. Journal of the Geological Society of London, v. 134, p. 269–292.

Sakata, S., 2018, A practical method for calculating the U-Pb age of Quaternary zircon: Correction for common Pb and initial disequilibria. Geochemical Journal, v. 52, p. 281–286.

Schmitz, M.D. and Bowring, S.A., 2001, U-Pb zircon and titanite systematics of the Fish Canyon Tuff: an assessment of high-precision U-Pb geochronology and its application to young volcanic rocks.

Geochimica et Cosmochimica Acta, v. 65, p. 2571–2587.

Sláma, J., Kosler, J., Condon, D.J., Crowley, J.L., Gerdes, A., Hanchar, J.M., Horstwood, M.S.A., Morris, G.A., Nasdala, L., Norberg, N., Schaltegger, U., Schoene, B., Tubrett, M.N., and Whitehouse, M.J., 2008, Plešovice zircon — A new natural reference material for U–Pb and Hf isotopic microanalysis. Chemical Geology, v. 249, p. 1–35.

Shervais, J.W., 2001, Birth, death, and resurrection: The life cycle of supra subduction zone ophiolites: Geochemistry, Geophysics, Geosystems, v. 2, Paper number 2000GC000080

Stern, R. J., and Bloomer, S. H., 1992, Subduction zone-infancy: Examples from the Eocene Izu-Bonin-Mariana and Jurassic California arcs: Geological Society of America Bulletin 104, 1621-1636.

Suga, K., 1994, Volcanic history of Higashiyama, Hachijojima. Bulletin of the Volcanological Society of Japan. Second series, v. 3, p. 13–2. (in Japanese with English abstract)

Suga, K., 1998, The evolution process and its characteristics in the Hachijojima volcanic group, Izu-Bonin Arc. The Quaternary Research, v. 39, p. 59–75. (in Japanese with English abstract)

Suga, K., Kawate, S., and Aoike, K., 1997, A few remarks on the growth history of Hachijojima Volcano, Izu-Bonin Islands. Bulletin of the Volcanological Society of Japan, Third series, v. 42, no. 227–231. (in Japanese with English abstract)

Suganuma, Y., Aoki, K., Kanamatsu, T., and Yamazaki, T., 2006, Tephrostratigraphy of deep-sea sediments in the northwestern Pacific and its implications for the chronology of the past 300 kyr. The Quaternary Research, v. 45. P. 435-450. (in Japanese with English abstract)

Sugihara, S., 1998, Tephrochronological study of Higashiyama Volcano at Hachijojima, Izu Islands. Journal of Geography, v. 107, p. 390–420. (in Japanese with English abstract)

Tamura, Y., Busby, C.J., Blum, P., Guèrin, G., Andrews, G.D.M., Barker, A.K., Berger, J.L.R., Bongiolo, E.M., Bordiga, M., DeBari, S.M., Gill, J.B., Hamelin, C., Jia, J., John, E.H., Jonas, A.-S., Jutzeler, M., Kars, M.A.C., Kita, Z.A., Konrad, K., Mahoney, S.H., Martini, M., Miyazaki, T., Musgrave, R.J., Nascimento, D.B., Nichols, A.R.L., Ribeiro, J.M., Sato, T., Schindlbeck, J.C., Schmitt, A.K., Straub, S.M., Vautravers, M.J., and Yang, Y., 2015, Expedition 350 summary. In Tamura, Y., Busby, C.J., Blum, P., and the Expedition 350 Scientists, Proceedings of the International Ocean Discovery Program, Expedition 350: Izu-Bonin-Mariana Rear Arc: College Station, TX (International Ocean Discovery Program).

Tsukui, M., Moriizumi, and M., Suzuki, M., 1991, Eruptive history of the Higashiyama Volcano, Hachijo Island during the last 22,000 years. Bulletin of the Volcanological Society of Japan, Second series, v. 36, p. 345–356. (in Japanese with English abstract)

Tsukui, M., Moriizumi, M., and Suzuki, M., 1993, Evolution of magma plumbing system of Hachiji-Higashiyama volcano in the last 30,000 years. Bulletin of the Volcanological Society of Japan, Second

series, v. 38, p. 199–212. (in Japanese with English abstract)

Tsukui, M., and Hoshino, K., 2002, Magmatic differentiation of Hachijo-Nishiyama volcano, Izu Islands, Japan. Bulletin of the Volcanological Society of Japan, Second series, v. 47, p. 57-72. (in Japanese with English abstract)

Yamamoto, H., and Aoki, K, 2002, Late Quaternary tephrostratigraphy in piston cores collected during "Mirai" MR00–K05 cruise. AMSTECR, v. 46, p. 29–36. (in Japanese with English abstract)

Yoshikawa, S., 1976, The volcanic ash layers of the Osaka Group. Journal of the Geological Society of Japan, v. 82, p. 497–515. (in Japanese with English abstract)

Yoshikawa, S., and Inouchi, Y., 1993, Middle Pleistocene to Holocene explosive volcanism revealed by ashes of the Takashima –oki core samples from Lake Biwa , Central Japan. The Association for the Geological Collaboration in Japan, v. 467, p. 97–109. (in Japanese with English abstract)

Tables

Tables 1-4 are available as downloads in the Supplementary Files section.

Figures

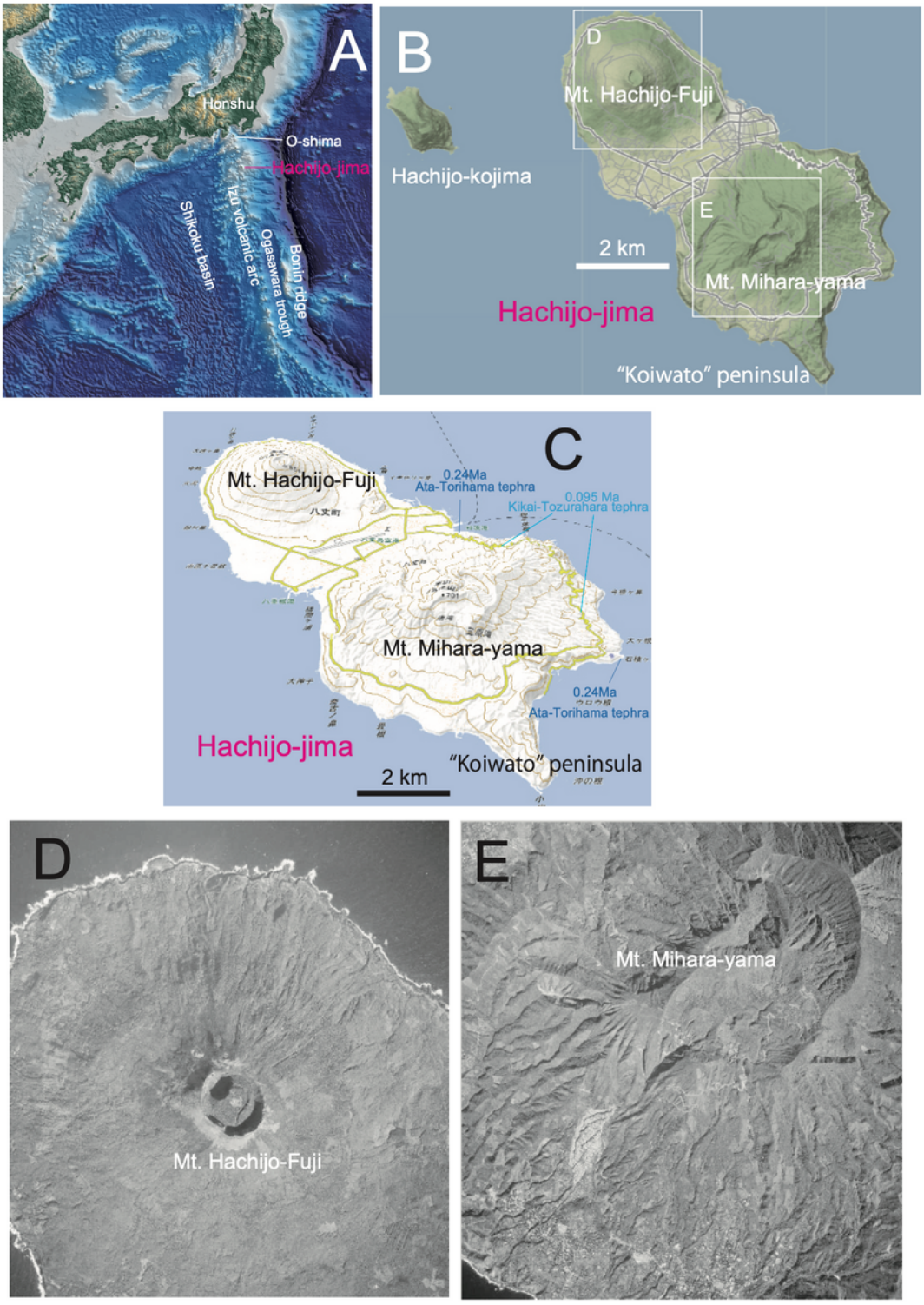

Figure 1

A: Index map of the Izu-Bonin arc (base map from Vector Map Level 0, National Geospatial-Intelligence Agency). B: Vector map of Hachijo-jima. C: 3D map of Hachijo-jima with tephra localities. D: Aerial photo of the Hachijo-Fuji volcano, not dissected. E: Aerial photo of the Mihara-yama volcano, severely dissected by post-eruptive erosion. Note that U-shaped deep valley and ridge is not a normal fault scarp of caldera, and the northeastern ridge is not a somma. Original volcanic structure (= stratovolcano) is not preserved.

Digital images of B ~ E from the Geospatial Information Authority of Japan. Note: The designations employed and the presentation of the material on this map do not imply the expression of any opinion whatsoever on the part of Research Square concerning the legal status of any country, territory, city or area or of its authorities, or concerning the delimitation of its frontiers or boundaries. This map has been provided by the authors.

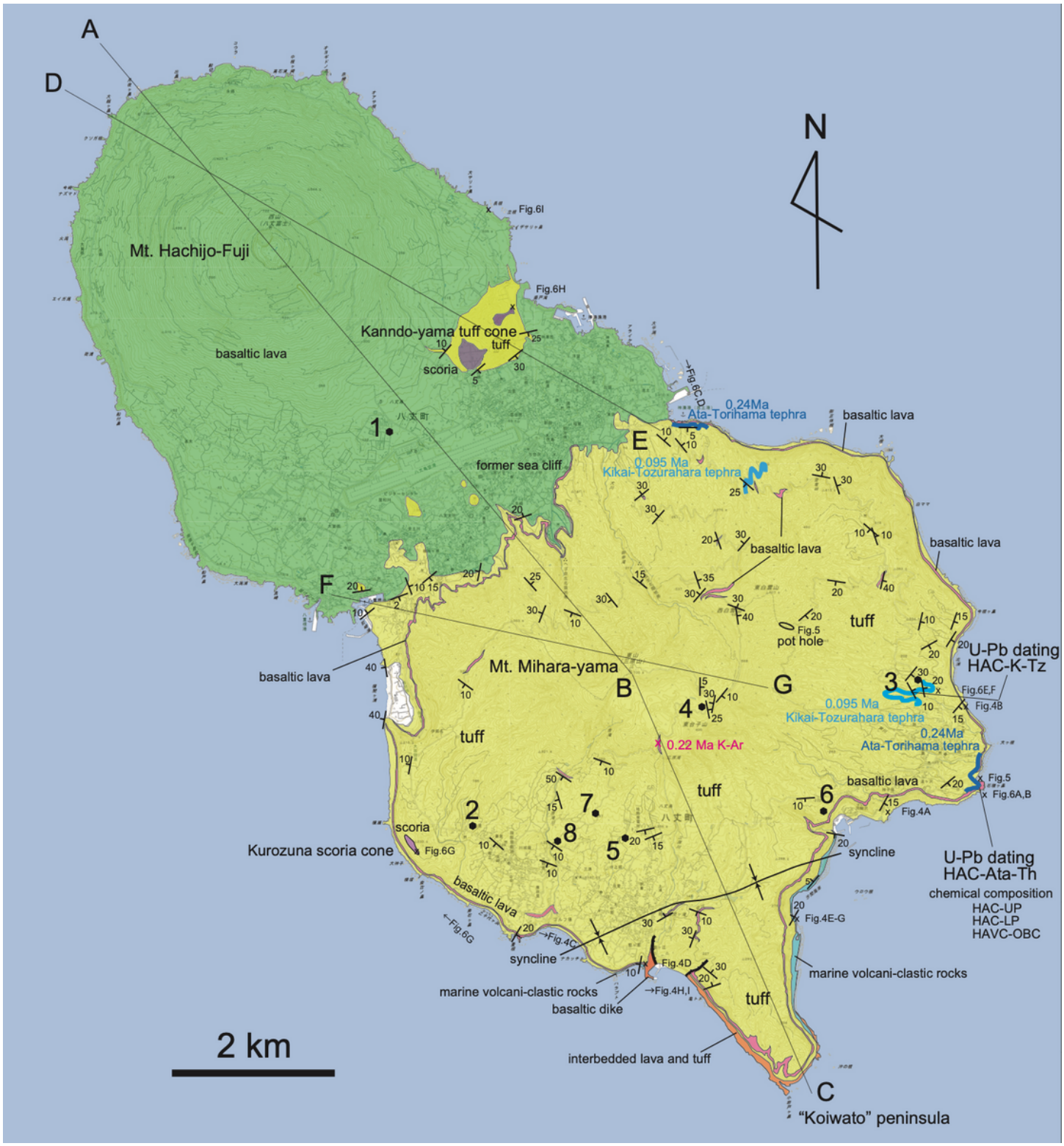

Figure 2

Geological map of Hachijo-jima. Numbered sites: bore holes by NEDO (1993). A-B-C, D-E, F-G: cross sections. Background: Digital topographic maps of 1: 25,000 scale, the Geospatial Information Authority of Japan. Note: The designations employed and the presentation of the material on this map do not imply the expression of any opinion whatsoever on the part of Research Square concerning the legal status of any country, territory, city or area or of its authorities, or concerning the delimitation of its frontiers or boundaries. This map has been provided by the authors.

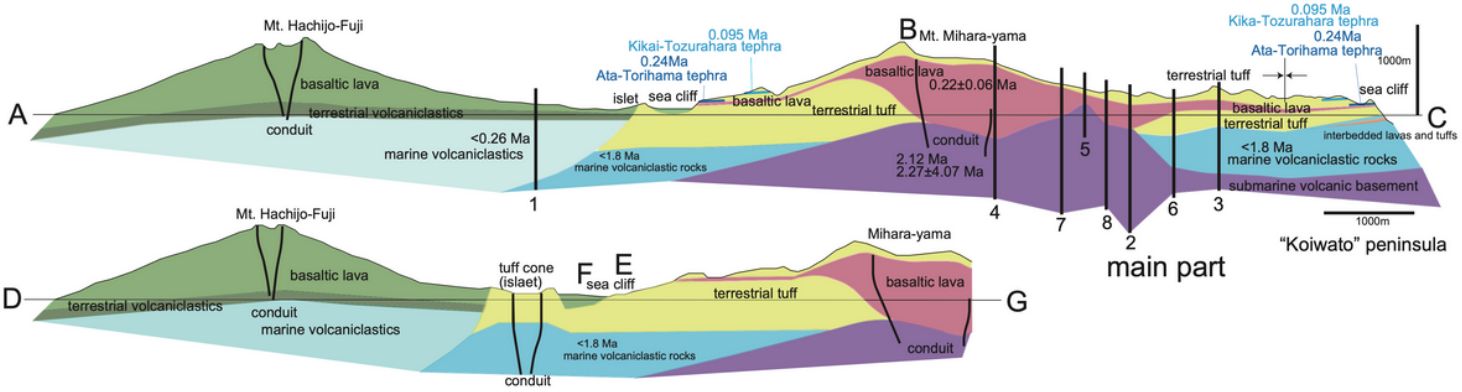

Figure 3

Geological cross sections. Drill core data from NEDO (1993) were used for the subsurface geology. U-Pb ages were obtained by the present study but represent the formal accepted dates (see text). Other K-Ar age data are from NEDO (1993) except for K-Ar date of 2.12 Ma from Kaneoka et al. (1970). The date of < 1.8 Ma for the marine volcaniclastic rocks of the Mihara-yama volcano is based on planktonic foraminifer datum, and the date of < 0.26 Ma for the marine volcaniclastic rocks of the Hachijo-Fuji volcano is based on calcareous nannoplankton datum (NEDO, 1993).

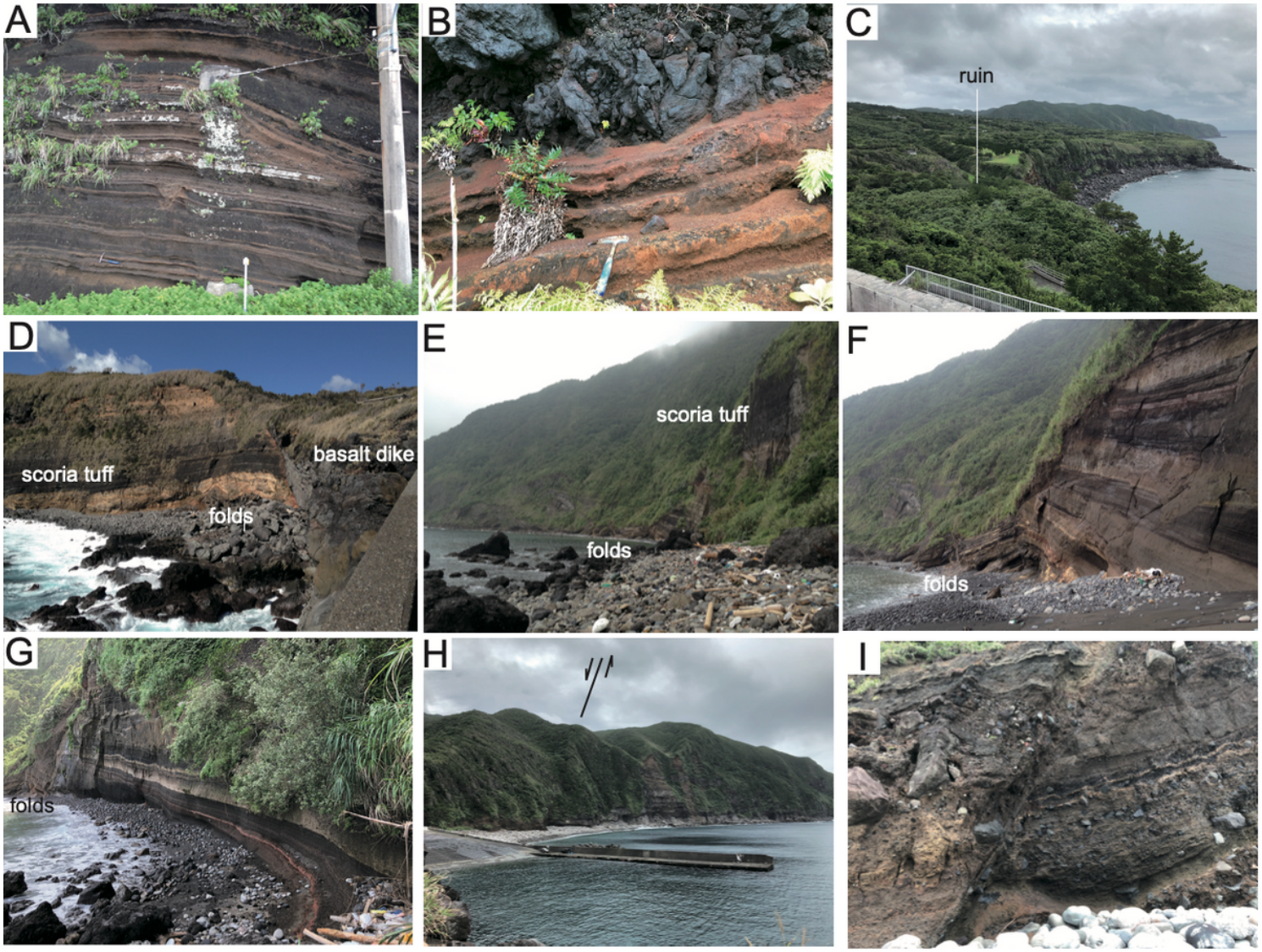

Figure 4

Outcrop photos. Photo localities are shown in Fig. 2. A: stratified scoriaceous tuff. B: key lava flow. Hematite was formed in the scoriaceous tuffs. C: A key basaltic lava flow along the sea cliff. Black key scoria tuff is visible at the base. Note that the dip is lower than that of the coastal slope. Another lava at the higher stratigraphic position than the cliff lava crops out within the vegetation, although Isshiki (1959) and Ishizuka and Geshi (2018) misinterpreted these as single lava flow that extended far inland. Ruins of human habitation were found, but these lack a systematic description of the occurrence of items as human bones, earthenware, and stone implements. The correlation to the 0.0073 Ma Kikai-Akahoya tephra (K-Ah; Sugihara, 1988; lacking descriptions relative to the ruins) is doubtful based on the age-stratigraphic information presented in this paper. D: The strata top of the cliff is light colored, but basaltic lava (key), below: black key scoria tuff of 10 m in thickness (extending from Fig. 4C), and below: asymmetrically folded and light colored bedded silicic and scoriaceous tuffs (key). These strata are cut by a basaltic intrusion (right side). The intrusion contact of the strata has an orientation of N10W 60NE and is reddish because of hematite growth. Isshiki (1959) and Ishizuka and Geshi (2018) described the dike as a lava flow from inland. E: Black key scoriaceous tuff of 10 m in thickness, and below: key

bedded silicic and scoriaceous tuffs, opposite eastern coast of the peninsula. Asymmetric folds are visible, as Fig. 4D. F: Close up of bedded silicic and scoriaceous tuffs and SSE vergent asymmetric folds. G: Close up, a grading from silicic tuff below to scoriaceous tuff above is visible, and the tuff contains obsidian. A hematite-rich tuff layer is intercalated. The white silicic tuff contained no zircon, so U-Pb dating of it was not possible. H: normal fault between tuff breccia (debris flow; hanging wall; left) and interbedded lava and tuff (foot wall; right). I: conjugate sets of normal faults in the hanging wall of a major normal fault ("main" fault). Orientation(s) of main fault: N30W 65SW; associated faults: N30W 55SW vs N30W 50NE, N10W 80SW, N10W 75SW (photo), three faults of N10W 60SW.

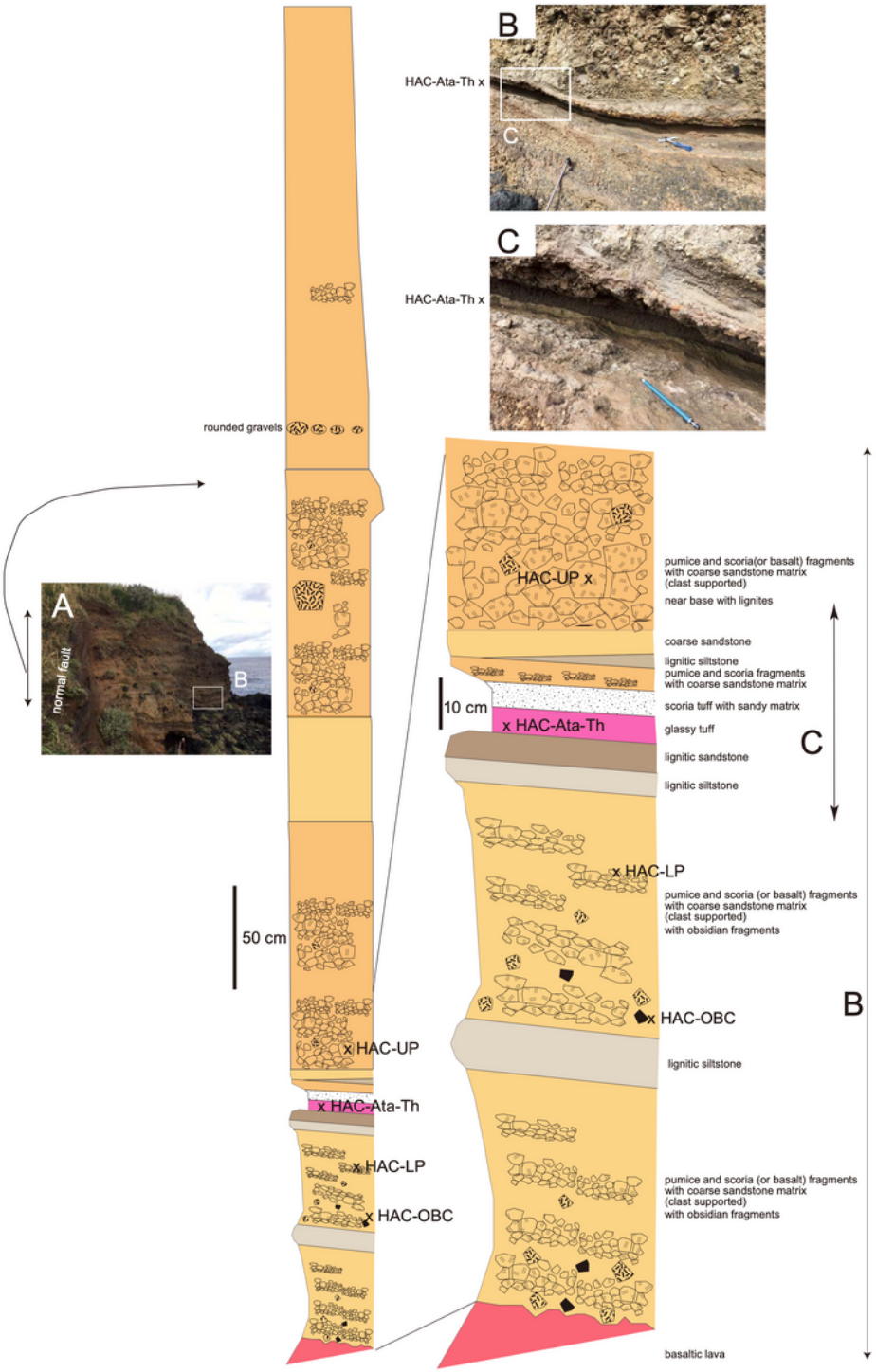

Figure 5

Columnar section and photos including the lower glassy tuff directly east of the Ishizumi-hana cape. HAC-Ata-Th of the glassy tuff specimen contains zircons of 50 to 200 μm, but HAC-UP and HAC-LP of pumice fragments contain no zircon. Both were geochemically analyzed including an obsidian fragment of HAC-OBC.

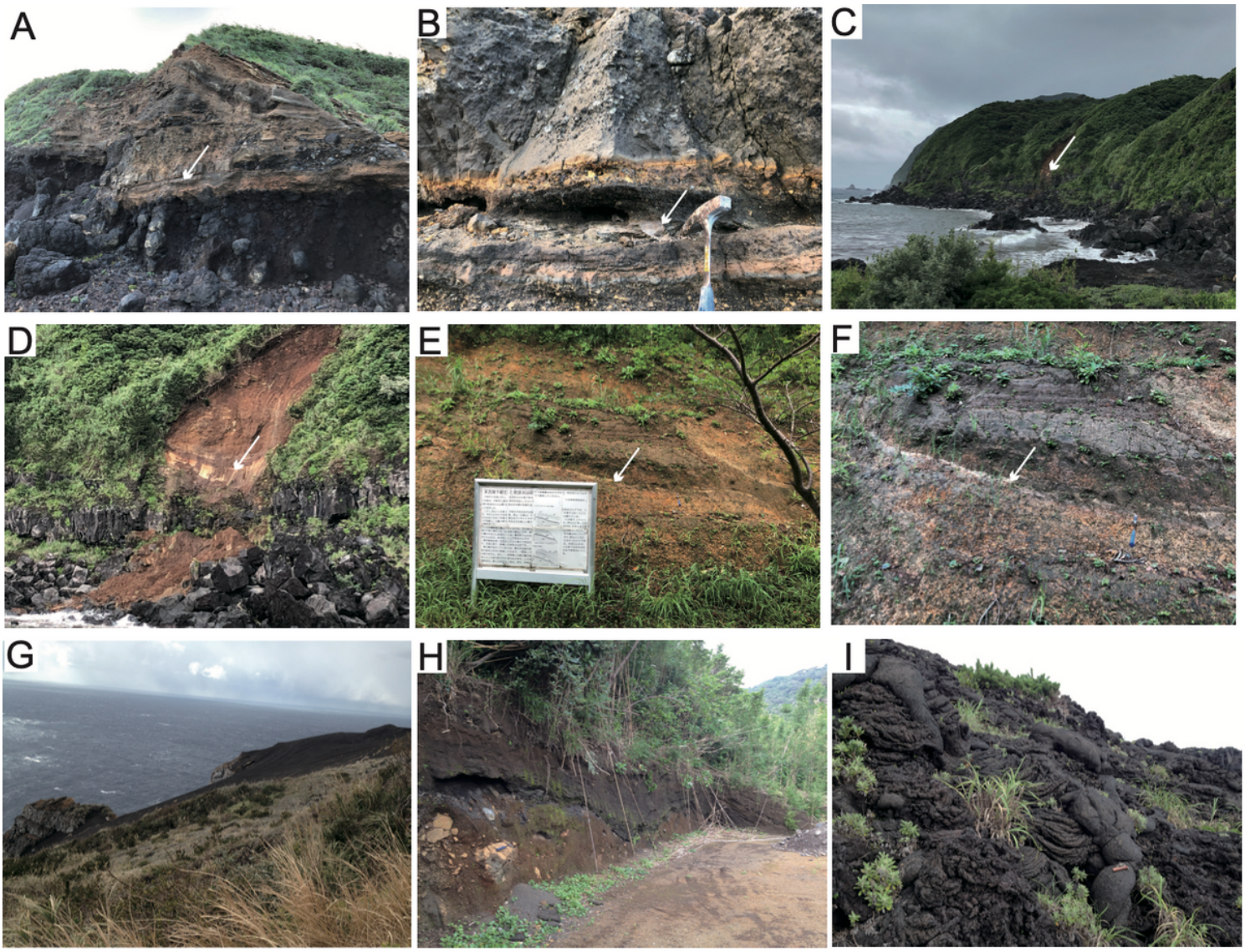

Figure 6

Outcrop photos. Photo localities are shown in Fig. 2. A: Lower glassy tuff (arrow) at the Ishizumi-hana cape, west of the cape (opposite side of Fig. 5) and directly above the key basaltic lava. To the NE on the cliff, the key basaltic lava with hematite-rich base is continuously exposed. B: close up. Arrow: glassy tuff. C: Lower silicic tuff (arrow) opposite side of the Sokodo port, directly above the key basaltic lava at the base of sea cliff. To the west (right and frontal side), the young, horizontally-oriented Hachijo-juji lava abuts the Mihara-yama key basaltic lava. D: close up of Fig. 4C. The white silicic tuff is very thick (2 m). E: The upper glassy tuff (arrow; HAC-K-Tz). Note that the strata dip to the SE (oceanward; to the right), and fresh hard tuff breccia located adjacent to the bridge southwest of the valley. The upper white line is a thrust fault associated with NW-vergent asymmetric fold to the right (SE side of the photo; not shown). The sign placed by the Board of Education in Hachijo-jima explains that the glassy tuff is the 0.02 Ma Aira-Tn tephra (which is incorrect; see text) intercalated in the unconsolidated (incorrect, see text) pumice falls from the Mihara-yama, and that the upper white line is an unconformity (incorrect as noted above). F: close up of Fig. 4E. G: Scoria cone (black) at the top of the sea cliff. “Kurosuna” (black sands) sightseeing locality. H: The Kando-yama scoria covers talus deposits. Tuff cone consists of tilted

scoriaceous tuff derived from the Mihara-yama volcano, not from the Hachijo-Fuji volcano. I: Pahoehoe lava of the Hachijo-Fuji volcano tilted oceanward.

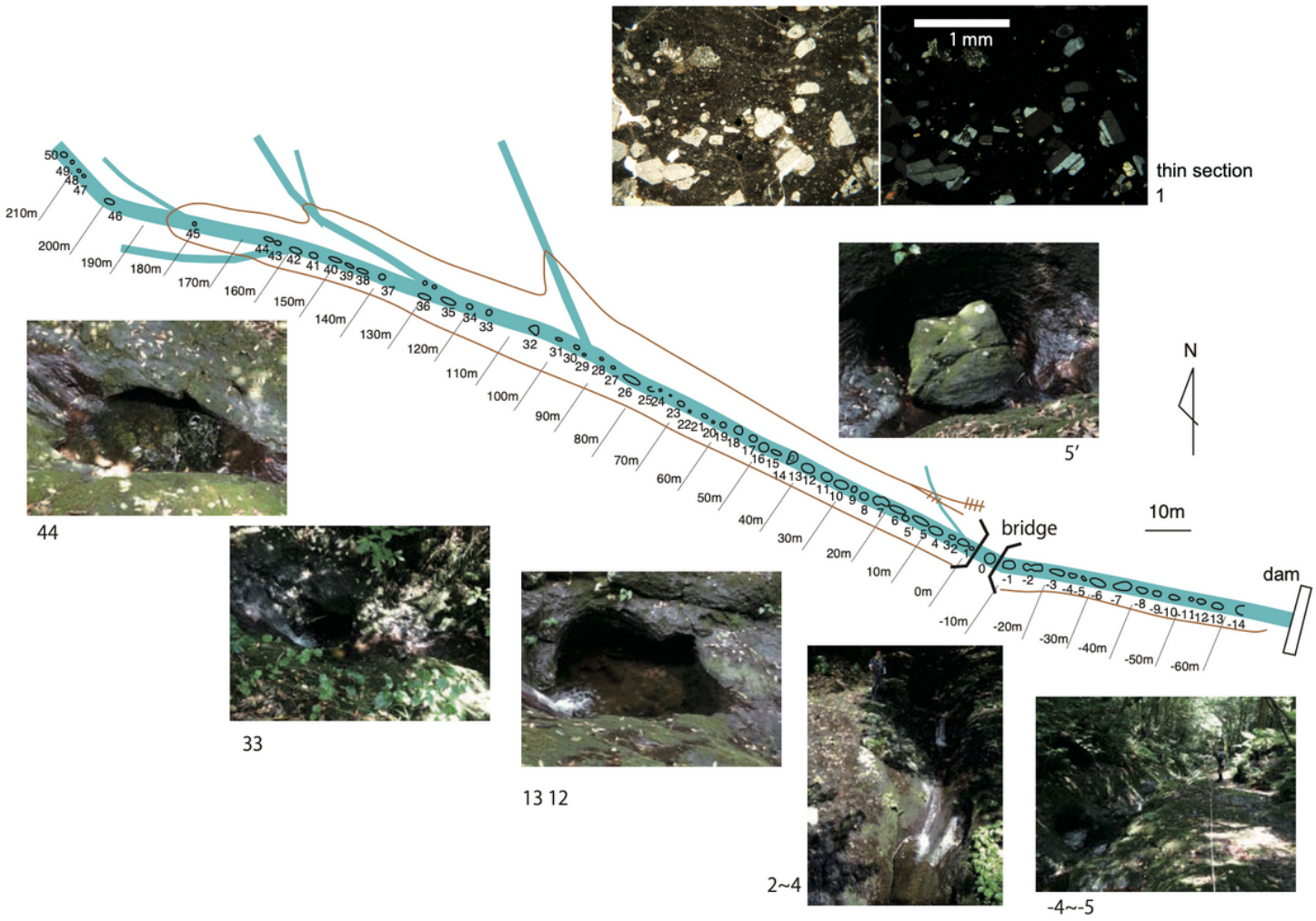

Figure 7

Route map of erosional streambed pot holes and associated field photos that illustrate the erosional resistance of the glassy tuffs; unconsolidated ash cannot form such erosional features. In addition, pbotomicrographs are presented with plane polarized and cross polarized views that show no welded structure. The pot hole transect area is shown in Fig. 2. Holes are numbered 0 at the bridge to 50 upstream of it, and downstream of it to -14.

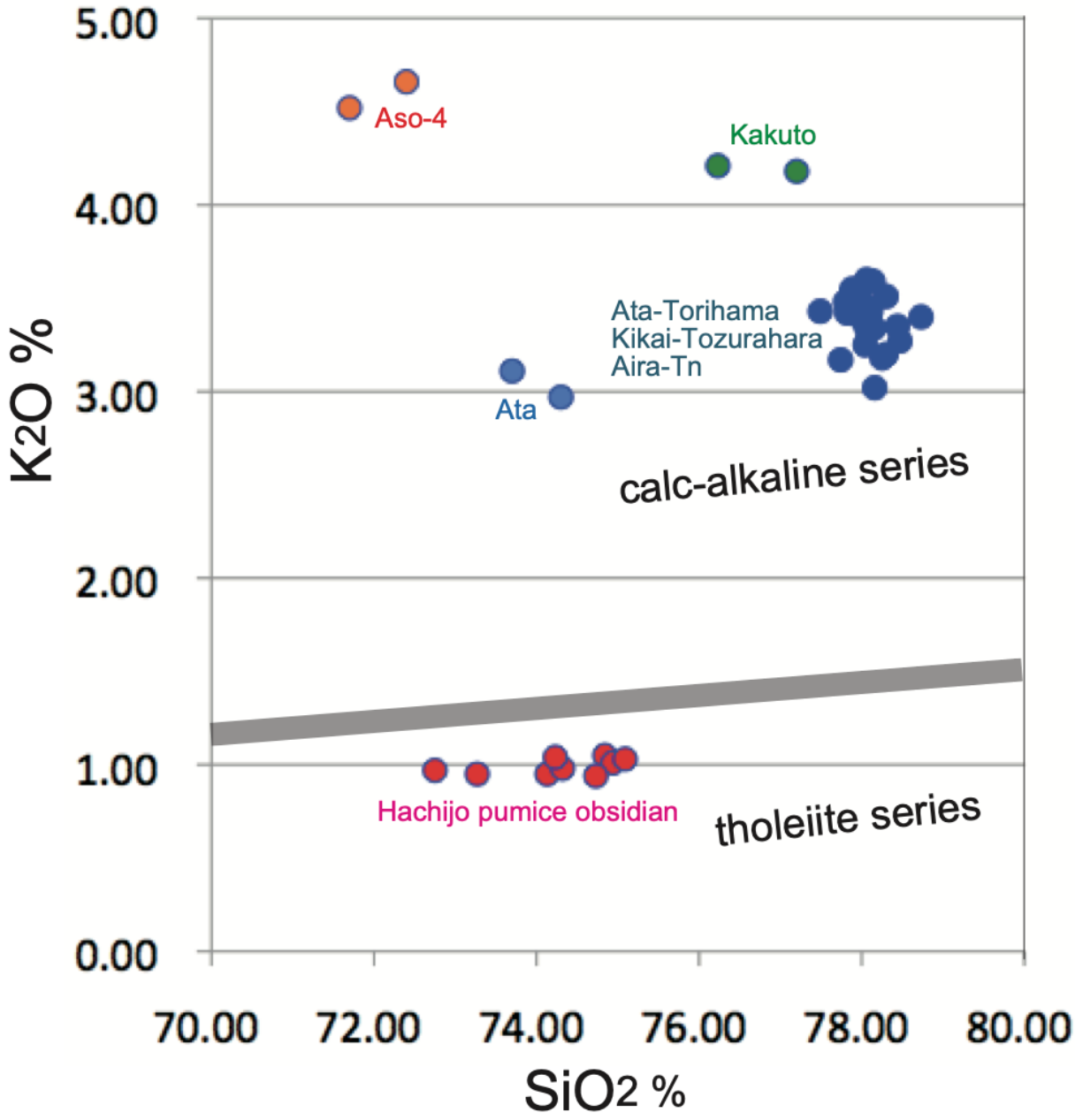

Figure 8

SiO2-K2O diagram made by Table 2 data. Ata-Torihama, Kikai-Tozurahara, and Aira-Tn tephras are clustered, and not discriminated by these elements. The Hachijo pumices in Fig. 5, and the Kakuto, Ata, and Aso-4 tephras are have distinct high K2O with lower SiO2. The tephras are plotted in the calc-alkaline series, and the Hachijo pumices are plotted in the tholeiite series.

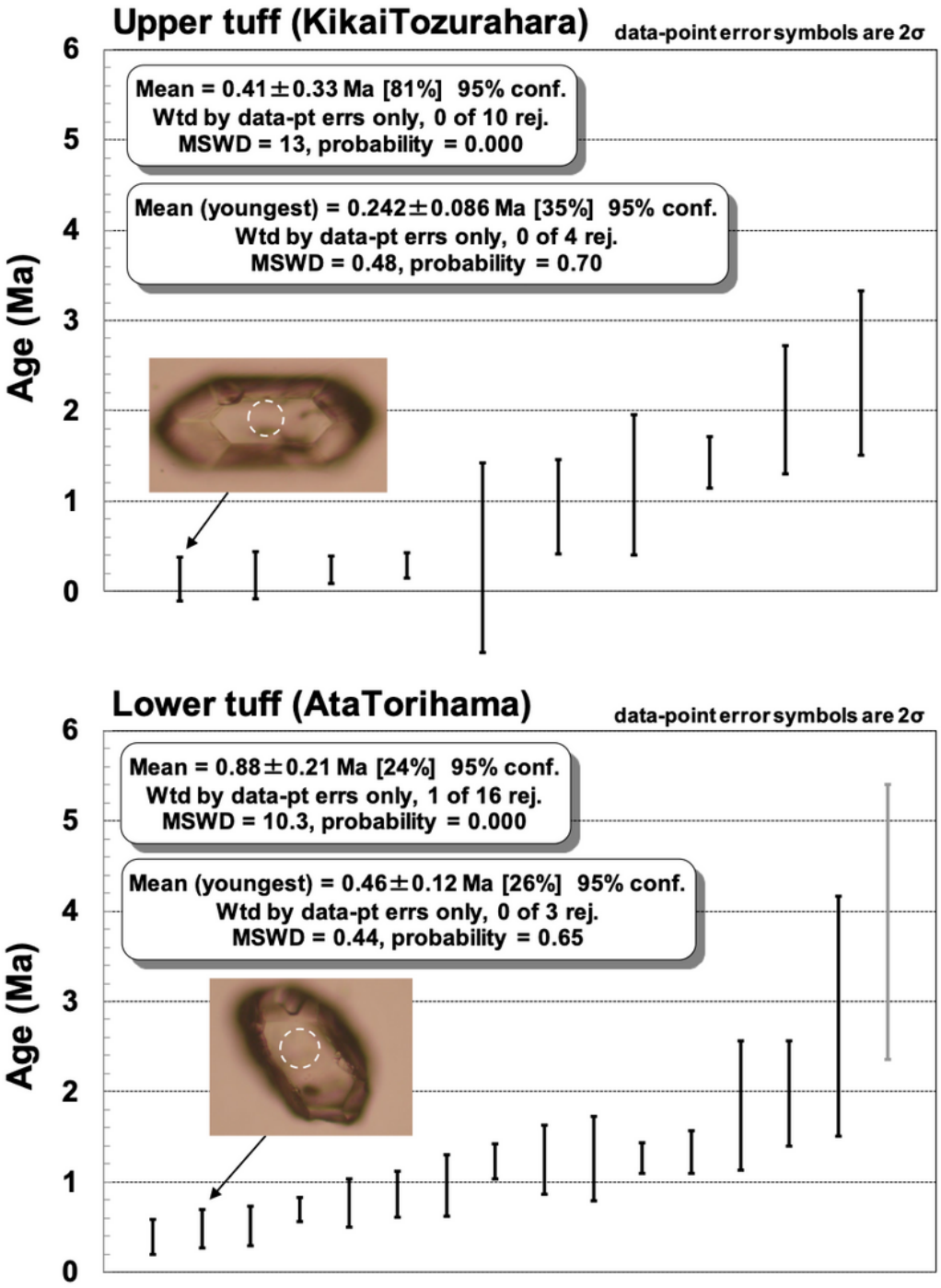

Figure 9

Zircon U-Pb ages (2σ analytical uncertainties) for the lower and upper glassy tuffs. Individual U-Pb grain ages are arranged from young to old. Also shown are photos of a typical zircon from each tuff. White dashed circles of 30μm diameter represent the positions of laser ablation.

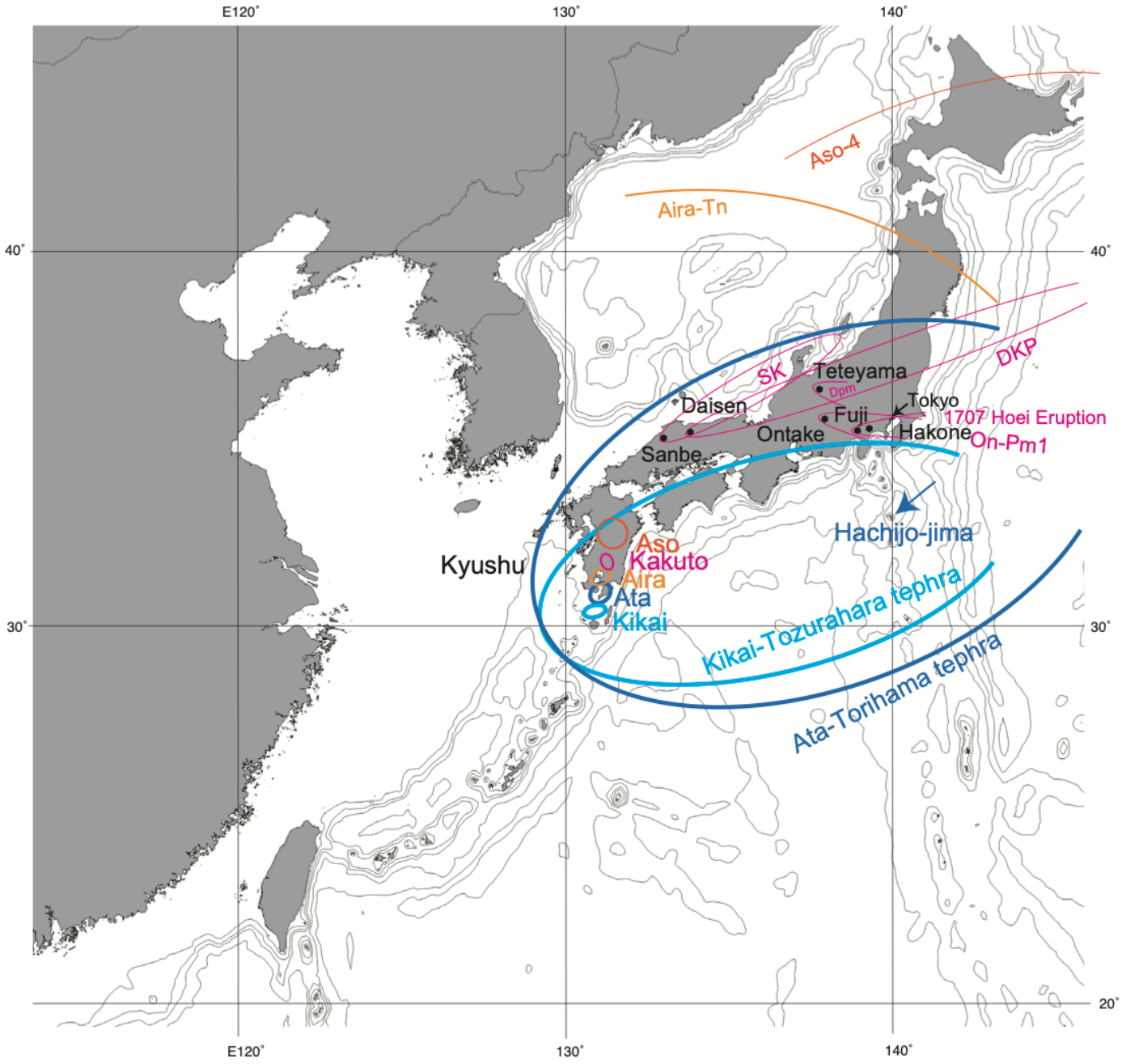

Figure 10

Regional map of the Ata-Torihama and Kikai-Tozurahara tephra source calderas and distributary pattern, and that of representative tephras of Machida and Arai (2003), as well as Sugenuma et al. (2006), Kasama and Shioi (2019), and references in Table 1 for the Ata-Th and K-Tz tephras. The Hoei Eruption in 1707, Mt. Fuji, from Disaster Management in Japan (also found in Wikipedia). The contour (curved colored lines) is a limit of ca. 5 cm in thickness, but for Aso-4 tephra: > 15 cm (Machida and Arai, 2003) and for Omachi (DPm) tephra: > 0cm (Ito and Danišík, 2020). Aso-4 tephra is found in northwest Pacific cores outside of Fig. 10 (Suganuma et al., 2006), representing the Aso ultra Plinian eruption. Aso-4 tephra, expected to exist just above the Kikai-Tozurahara tephra, was not found from the upper Mihara-yama

succession, and the Mihara-yama age should be < 0.0875 Ma (date of Aso-4; Table 1). Note: The designations employed and the presentation of the material on this map do not imply the expression of any opinion whatsoever on the part of Research Square concerning the legal status of any country, territory, city or area or of its authorities, or concerning the delimitation of its frontiers or boundaries. This map has been provided by the authors.

Supplementary Files

This is a list of supplementary files associated with this preprint. Click to download.

- Table1ListTephra.png
- Table2ChemCompSheet1.png
- Table3UPb.png
- Table4IsArea.xlsx